Controlled-Deactivation Cannabinergic Ligands

ARTICLE *in* JOURNAL OF MEDICINAL CHEMISTRY · NOVEMBER 2013

Impact Factor: 5.45 · DOI: 10.1021/jm4016075 · Source: PubMed

Journal of Medicinal Chemistry

Article

pubs.acs.org/jmc

Controlled-Deactivation Cannabinergic Ligands

Rishi Sharma,[†,§] Spyros P. Nikas,*[,†] Carol A. Paronis,[†] JodiAnne T. Wood,[†] Aneetha Halikhedkar,[†] Jason Jianxin Guo,[†] Ganesh A. Thakur,[†] Shashank Kulkarni,[†] Othman Benchama,[†] Jimit Girish Raghav,[†] Roger S. Gifford,[†] Torbjörn U. C. Järbe,[†] Jack Bergman,[‡] and Alexandros Makriyannis*[,†]

[†]Center for Drug Discovery and Departments of Chemistry and Chemical Biology and Pharmaceutical Sciences, Northeastern University, Boston, Massachusetts 02115, United States

[‡]McLean Hospital, Harvard Medical School, Belmont, Massachusetts 02478, United States

Supporting Information

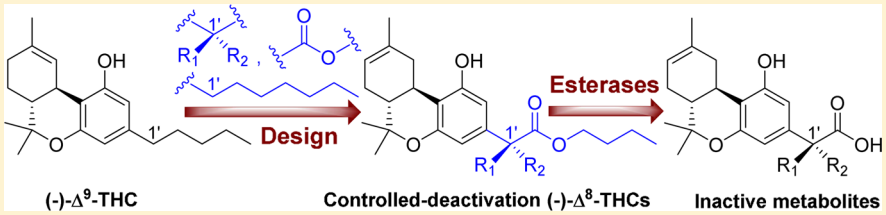

ABSTRACT: We report an approach for obtaining novel cannabinoid analogues with controllable deactivation and improved druggability. Our design involves the incorporation of a metabolically labile ester group at the 2′-position on a series of (−)-Δ^8-THC analogues. We have sought to introduce benzylic substituents α to the ester group which affect the half-lives of deactivation through enzymatic activity while enhancing the affinities and efficacies of individual ligands for the CB1 and CB2 receptors. The 1′-(*S*)-methyl, 1′-*gem*-dimethyl, and 1′-cyclobutyl analogues exhibit remarkably high affinities for both CB receptors. The novel ligands are susceptible to enzymatic hydrolysis by plasma esterases in a controllable manner, while their metabolites are inactive at the CB receptors. In further in vitro and in vivo experiments key analogues were shown to be potent CB1 receptor agonists and to exhibit CB1-mediated hypothermic and analgesic effects.

INTRODUCTION

(−)-Δ^9-Tetrahydrocannabinol[1] [(−)-Δ^9-THC, **1**, Figure 3] and its structural analogues produce most of their physiological effects by interacting with the CB1 and CB2 cannabinoid (CB) receptors.[2−5] Modulation of these GPCRs is a promising pharmacotherapeutic strategy for treating various conditions including pain, neurodegeneration, inflammation, glaucoma, and eating disorders.[6−12] However, only a limited number of cannabinergic drugs including dronabinol (synthetic Δ^9-THC), nabilone (Δ^9-THC analogue), and Sativex (mixture of Δ^9-THC and cannabidiol) have been developed to date. The difficulties involved in the development of such therapeutically useful medications are due to the undesirable side effects associated with CB1 receptor activation which include CNS and cardiovascular effects, abuse potential, poor oral bioavailability, and unpredictable time course of action and detoxification.[13] For example, oxidative metabolism of Δ^9-THC by cytochrome 450 generates 11-hydroxy-Δ^9-THC, which is a potent psychoactive cannabinoid with a very long pharmacological half-life.[14,15] Therefore, there is still a need for the development of safer THC-based analogues/drugs with good oral bioavailability, consistent efficacy, and predictable duration of action and detoxification.

The "soft analogue/drug" approach has been used successfully to improve pharmacokinetic and pharmacodynamic (PK/PD) profiles as well as specificity for a variety of drug targets, such as anticholinergics, β-blockers, corticosteroids, and opioids.[16−18] In general, soft analogues/drugs are bioactive analogues of a lead compound/drug that have a metabolically labile feature built into their structures. They are designed to undergo a predictable and controllable deactivation to inactive metabolites after the desired biological/pharmacological role has been achieved (Figure 1).

The therapeutic potential of soft cannabinergic agonists found application in a number of conditions such as glaucoma, perioperative and postoperative pain, and drug addiction. Earlier efforts to incorporate a metabolically vulnerable ester group at the side chain of a biphenyl cannabimimetic ligand led to compounds with very low affinity for CB receptors.[19] In a different approach, ester group containing *N*-benzylbenzopyrones that share some structural features with nabitan, a cannabinoid lead developed at Abbott Laboratories, were synthesized.[12,20] Although CB receptor binding affinities and cannabinoid related behavioral pharmacology of these compounds are not reported, in vivo testing suggests that they possess moderate intraocular pressure lowering activity.[12]

In this communication, we have combined the soft drug concept of enzymatic deactivation with a "depot effect" that has been frequently observed with the generally hydrophobic

Received: October 16, 2013

   dx.doi.org/10.1021/jm4016075 | *J. Med. Chem.* XXXX, XXX, XXX−XXX

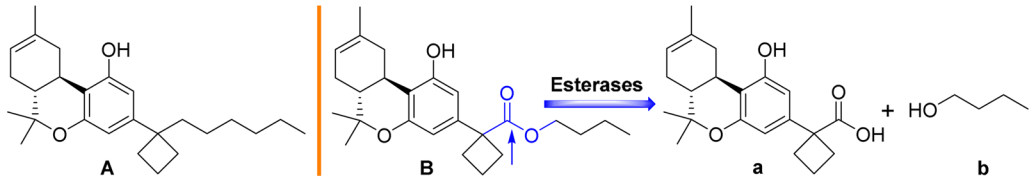

Figure 1. Example of controlled-deactivation cannabinergic ligand. Compound **A** [AMG38, (6aR-*trans*)-3-(1-hexylcyclobutyl)-6a,7,10,10a-tetrahydro-6,6,9-trimethyl-6*H*-dibenzo[*b*,*d*]pyran-1-ol][23] is a potent CB1 receptor agonist (K_i = 1.5 nM), while compound **B** (**2e**) is its corresponding analogue with similar pharmacophoric groups while also encompassing a key ester group in its side chain which is available for enzymatic cleavage. Through the action of esterases, **B** yields two fragments (**a** and **b**) that are shown to have negligible cannabinergic activity.

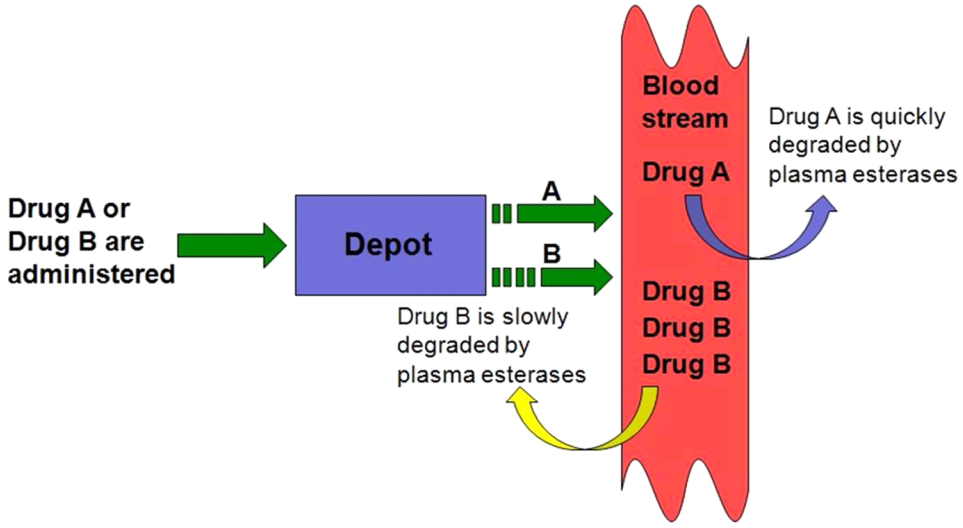

Figure 2. Control of drug activity through esterase actions and depot effects. Compounds similar to drug A (less lipophilic, quickly hydrolyzable) are sequestered in fatty tissues followed by release in the bloodstream and rapid inactivation by plasma esterases. Compounds similar to drug B (more lipophilic, slowly hydrolyzable) are more slowly released in the bloodstream from the depot and more slowly inactivated by plasma esterases. The rate of enzymatic inactivation of A and B is dependent on structural features in the vicinity of the hydrolyzable group. By incorporating features modulating these two parameters (depot effect, enzymatic action), we can obtain ligands with controllable half-lives.

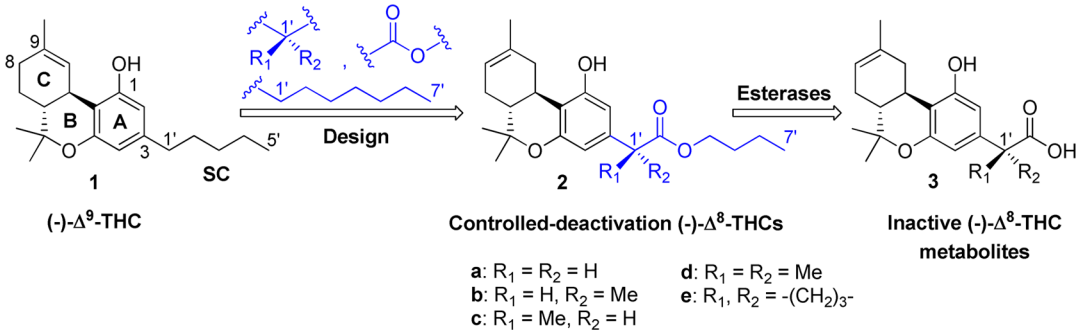

Figure 3. Design of (−)-Δ[8]-tetrahydrocannabinols with controllable deactivation and structures of the lead compound (−)-Δ[9]-THC and inactive metabolites.

cannabinergic compounds. In our controlled deactivation design, the ligand's systemic half-life is determined by two factors (Figure 2). The first is the extent to which the ligand is sequestered within the body before it is released for systemic circulation (depot effect). This process is dependent on the compound's physicochemical properties and can be modulated by adjusting log *P* and PSA. The second parameter is the rate of enzymatic hydrolysis by blood esterases. This can be calibrated by incorporating suitable stereochemical features in the vicinity of the hydrolyzable group (enzymatic effect). For the current work, which involves the design of cannabinoid analogues with controllable deactivation and improved druggability, we chose the well-known tetrahydrocannabinol template (THC). Detailed Δ[8]-THC structure−activity relationship (SAR) studies have shown that the aliphatic side chain (SC) at C3 plays a pivotal role in determining the cannabinergic potency of THCs.[5,21,22] Also, we and others have provided evidence that substituents at 1′-position can play a significant role in determining the compound's ability to interact with CB receptors.[21,23−27] On the basis of the above, we incorporated a metabolically labile ester group within the side chain pharmacophore of the THC structure. In such a design the carboxylic acid metabolite **3** (Figure 3) resulting after enzymatic hydrolysis was expected to have no activity at the

dx.doi.org/10.1021/jm4016075 | *J. Med. Chem.* XXXX, XXX, XXX−XXX

Scheme 1[a]

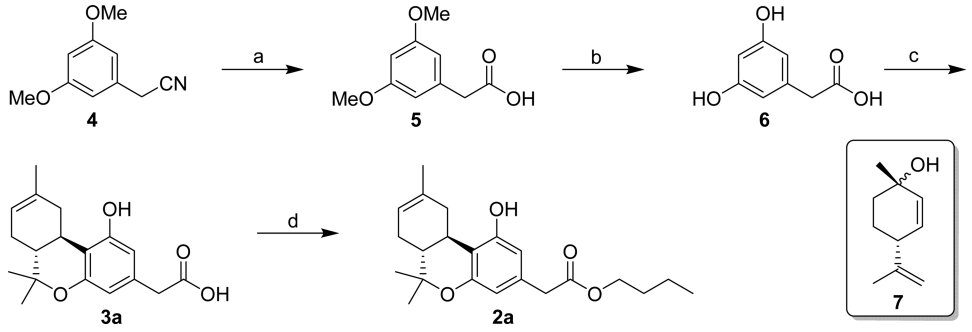

[a]Reagents and conditions: (a) NaOH, *n*-BuOH/H_2O (2:1), reflux, 4 h, 89%; (b) BBr_3, CH_2Cl_2, −78 °C to rt, 7 h, 88%; (c) (+)-*cis*/*trans*-*p*-mentha-2,8-dien-1-ol (**7**), *p*-TSA, $CHCl_3$, reflux 6 h, 40%; (d) $CH_3(CH_2)_3Br$, $NaHCO_3$, DMF, microwave irradiation, 165 °C, 12 min, 61%.

Scheme 2[a]

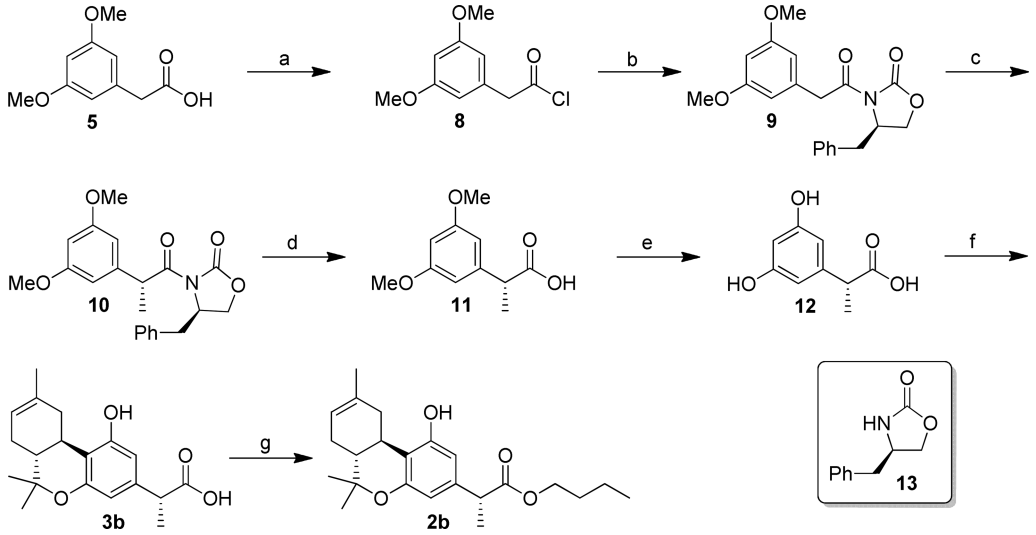

[a]Reagents and conditions: (a) $SOCl_2$, 1*H*-benzotriazole, CH_2Cl_2, rt, 20 min, 92%; (b) (*R*)-4-benzyloxazolidin-2-one (**13**), *n*-BuLi, −30 °C, 30 min, then addition of **8**, −30 °C to rt, 4 h, 66%; (c) $(Me_3Si)_2N^-Na^+$, MeI, −78 to −30 °C, 3 h, 63%; (d) LiOH, THF/H_2O (1:1), 0 °C, 2 h, 50%; (e) BBr_3, CH_2Cl_2, −78 °C to rt, 7h, 73%; (f) (+)-*cis*/*trans*-*p*-mentha-2,8-dien-1-ol (**7**), *p*-TSA, $CHCl_3$, reflux 6 h, 40%; (g) $CH_3(CH_2)_3Br$, $NaHCO_3$, DMF, microwave irradiation, 165 °C, 12 min, 67%.

CB receptors. In addition, we have incorporated α to the ester moiety methyl, geminal dimethyl, and cyclobutyl groups at the C1′ carbon to explore the role of steric factors on the rate of enzymatic deactivation of the novel enzymatically labile analogues. As with earlier work, we used (−)-Δ^8-THC as our prototype, favoring it over the less stable and almost equipotent isomer (−)-Δ^9-THC, while the length of the side chain was optimized to seven atoms. Overall, our design maintains the optimized pharmacophoric features of the lead compound while favoring the hydrolytic deactivation step over the preferred oxidative P450-based liver metabolism of prototypic cannabinoids. Such a design maintains control over the pharmacological half-life of the novel analogues while avoiding the potentially confounding roles of biologically active metabolites.

All synthesized analogues were characterized biochemically by determining their in vitro CB1 and CB2 receptor affinities, functional activities, and assessment of their in vitro metabolic stability toward mouse and rat plasma esterases. The in vitro results validated the stereochemical considerations used in the design of the novel ester side chain analogues. Equally important, the presence of an ester group within the cannabinoid side chain maintained or exceeded the ability to favorably interact with both receptors when compared with their all-carbon side chain counterparts.

Of the compounds described here, those with methyl, geminal dimethyl, and cyclobutyl substituents at C1′ were shown to exhibit remarkably high affinities for CB1 and CB2 receptors (6.2 nM > K_i > 0.3 nM). They are also susceptible to enzymatic hydrolysis by plasma esterases in a controllable manner, while their metabolites did not significantly interact with the CB receptors. Further in vitro and in vivo characterization suggested that three of the analogues identified in this study are potent CB1 receptor agonists (4.2 nM > EC_{50} > 0.4 nM) and exhibit CB-mediated hypothermic effects. Also, in both the hypothermia and analgesia assays the side chain ester analogue with the geminal dimethyl group at C1′ showed a faster onset and shorter duration of action than the all-carbon side chain counterpart Δ^8-THC-DMH. The SAR results for this series of novel cannabinergic analogues are also discussed using molecular modeling of key analogues.

dx.doi.org/10.1021/jm4016075 | *J. Med. Chem.* XXXX, XXX, XXX−XXX

Scheme 3[a]

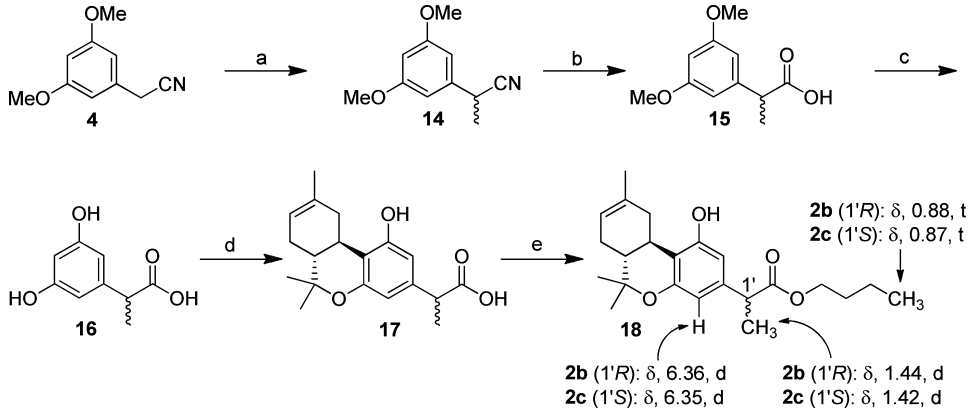

[a]Reagents and conditions: (a) NaH, MeI, DMF, −78 °C, 15 min then rt, 2 h, 75%; (b) NaOH, *n*-BuOH/H_2O (2:1), reflux, 4 h, 92%; (c) BBr_3, CH_2Cl_2, −78 °C to rt, 7 h, 78%; (d) (+)-*cis*/*trans*-*p*-mentha-2,8-dien-1-ol (**7**), *p*-TSA, $CHCl_3$, reflux 6 h, 46%; (e) $CH_3(CH_2)_3Br$, $NaHCO_3$, DMF, microwave irradiation, 165 °C, 12 min, 71%.

Scheme 4[a]

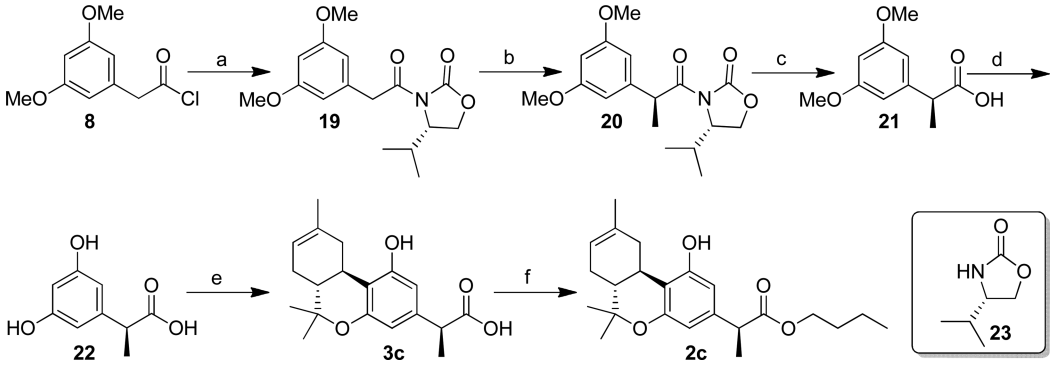

[a]Reagents and conditions: (a) (*S*)-4-isopropyloxazolidin-2-one (**23**), *n*-BuLi, −30 °C, 30 min, then addition of **8**, −30 °C to rt, 4 h, 65%; (b) $(Me_3Si)_2N^-Na^+$, MeI, −78 to −30 °C, 3 h, 82%; (c) LiOH, THF/H_2O (1:1), 0 °C, 2 h, 90%; (d) BBr_3, CH_2Cl_2, −78 °C to rt, 7 h, 79%; (e) (+)-*cis*/*trans*-*p*-mentha-2,8-dien-1-ol (**7**), *p*-TSA, $CHCl_3$, reflux 4 h, 41%; (f) $CH_3(CH_2)_3Br$, $NaHCO_3$, DMF, microwave irradiation, 165 °C, 12 min, 63%.

CHEMISTRY

Generally, the key step in the synthesis of side chain ester congeners of Δ^8-THC (**2a**−**e**) involves condensation of the chiral monoterpenoid alcohol (+)-*cis*/*trans*-*p*-mentha-2,8-dien-1-ol (**7**) with an appropriately 5-substituted resorcinol in the presence of *p*-toluenesulfonic acid.[28,29] This one step, acid catalyzed stereoselective process involves three consecutive reactions: (1) a Friedel−Crafts allylation, (2) a dibenzopyran ring closure, and (3) a Δ^9 to Δ^8 double bond isomerization.[23−25,30]

Synthesis of the (−)-Δ^8-THC ester derivative **2a** is depicted in Scheme 1. Hydrolysis of commercially available (3,5-dimethoxyphenyl)acetonitrile (**4**) under basic conditions afforded acid **5** (89% yield) which was then demethylated using boron tribromide to give resorcinol **6** in 88% yield. Acid catalyzed condensation of this intermediate with chiral **7** in refluxing chloroform produced (−)-Δ^8-THC acid **3a** in 40% yield. Alkylation of the respective carboxylate anion with 1-bromobutane under microwave heating led to the corresponding ester **2a** in 61% yield requiring short reaction times (12 min).

Construction of the (1′*R*)-Me-(−)-Δ^8-THC ester **2b** is shown in Scheme 2. Treatment of acid **5** with thionyl chloride/benzotriazole[31] furnished acyl chloride **8** (92% yield). Deprotonation of Evan's chiral auxiliary **13**[32,33] with *n*-BuLi followed by N-acylation with **8** led to oxazolidinone imide **9** in 66% yield. Enolization of **9** with sodium bis(trimethylsilyl)-amide at −78 °C and treatment of the resulting enolate with methyl iodide (−78 to −30 °C) afforded the methylated imide **10** in good yield (63%).[34,35] Subsequent hydrolysis of **10** under mild basic conditions[34,35] led to resorcinol dimethyl ether **11** (50% yield) which was treated with boron tribromide[23,26] to give the corresponding resorcinol **12** in 73% yield. Condensation of **12** with the monoterpenoid alcohol **7** provided the precursor acid **3b** (40% yield) which upon treatment with 1-bromobutane and sodium bicarbonate under microwave heating gave the respective ester **2b** in 67% yield.

To determine the stereoselectivity of our approach, an equally populated diastereomeric mixture **18** was synthesized and its ^{1}H NMR (500 MHz) spectrum was used to identify differences in the proton signals of the two diastereomers (**2c** and **2b**, Scheme 3). Subsequently, analysis of the ^{1}H NMR spectrum of the product obtained during the stereoselective synthesis of **2b** (Scheme 2) showed that the ratio **2b**/**2c** was 92:8. For testing and analytical purposes, pure **2b** was isolated after purification of the reaction mixture by flash column chromatography.

The diastereomeric mixture **18** was synthesized from nitrile **4** as shown in Scheme 3. Briefly, deprotonation at −78 °C and

dx.doi.org/10.1021/jm4016075 | J. Med. Chem. XXXX, XXX, XXX−XXX

Scheme 5[a]

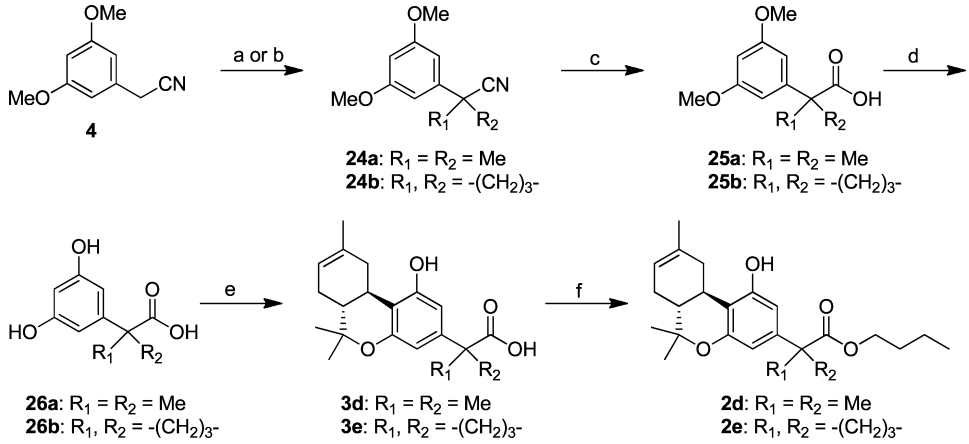

[a]Reagents and conditions: (a) NaH, MeI, DMF, 0 °C, 15 min, then rt, 2 h, 95% for **24a**; (b) $(Me_3Si)_2N^-K^+$, $Br(CH_2)_3Br$, THF, −16 °C, 2 h, 55% for **24b**; (c) NaOH, *n*-BuOH/H_2O (2:1), reflux, 4 h, 88−93%; (d) BBr_3, CH_2Cl_2, −78 °C to rt, 7 h, 85−87%; (e) (+)-*cis*/*trans*-*p*-mentha-2,8-dien-1-ol (**7**), *p*-TSA, $CHCl_3$, reflux 6 h, 39−45%; (f) $CH_3(CH_2)_3Br$, $NaHCO_3$, DMF, microwave irradiation, 165 °C, 12 min, 67−68%.

quenching with methyl iodide afforded the monomethylated nitrile **14** (75%). Nitrile hydrolysis followed by deprotection of the phenolic hydroxyl groups and coupling with **7** led to acid **17** which upon microwave assisted esterification gave **18**.

Stereoselective synthesis of the (1′*S*)-Me-(−)-Δ^8-THC diastereomer (**2c**) was accomplished using the oxazolidinone chiral auxiliary **23**[35] (Scheme 4). In a similar fashion, acyl chloride **8** was transformed into the desired 2*S*-propanoic acid derivative **21** following literature precedent.[35] This involves acylation of **23** (65%) followed by asymmetric methylation (82%) and saponification (90%). Starting from acid **21**, the sequence deprotection, terpenylation, esterification worked as expected and produced diastereomer **2c** in good overall yield. Again, a comparison of the ^{1}H NMR (500 MHz) spectrum of the diastereomeric mixture **18** with that of the crude product obtained during the stereoselective synthesis of **2c** showed that the stereoselection **2c**/**2b** was 91:9. This indicates that both the benzyl- and the isopropyl-substituted chiral auxiliaries **13** and **23** worked equally well leading to similar stereochemical outcomes.

The syntheses of the 1′-*gem*-dimethyl and the 1′-cyclobutyl analogues **2d** and **2e** are summarized in Scheme 5. Sequential deprotonation of **4** with sodium hydride and geminal dimethylation using methyl iodide at 0 °C gave **24a** in excellent yield (95%) and free from the monomethylated product **14**. Following the methodology we reported earlier,[23−25,36,37] cyclo-bis-alkylation of the starting nitrile **4** using potassium bis(trimethylsilyl)amide and 1,3-dibromopropane afforded **24b**. Alkaline hydrolysis of nitriles **24a** and **24b** (88−93% yield) and cleavage of the ether groups in **25a** and **25b** (85−87% yield) followed by terpenylation of resorcinols **26a** and **26b** (39−45% yield) and esterification (67−78% yield) of the intermediate acids **3d** and **3e** led to the respective (−)-Δ^8-THCs **2d** and **2e**.

Overall, key steps in the stereospesific syntheses of the side chain ester analogues involve (1) acid catalyzed condensation of a 5-substituted resorcinol with (+)-*cis*/*trans*-*p*-mentha-2,8-dien-1-ol, (2) asymmetric methylation using chiral auxiliaries, and (3) microwave assisted esterification.

RESULTS AND DISCUSSION

Cannabinoid Receptor Binding Studies. The abilities of **2a−e** and **3a−3e** to displace radiolabeled CP-55,940 from membranes prepared from rat brain (source of CB1 receptor) and HEK 293 cells expressing mouse CB2 receptor were determined as described in the Experimental Section,[23,26] and inhibition constants (K_i) from the respective competition binding curves are listed in Table 1. The compounds included in this study are optimized (−)-Δ^8-THC analogues in which a seven atom long side chain, with or without 1′-substituents, carry a 2′,3′-ester group. As expected, the hydrolytic metabolites **3a−e** have no significant affinity for CB receptors. Comparison of the binding data of (−)-Δ^8-THC and its analogue **2a** suggests that extension of the chain from five to seven atoms along with incorporation of an ester group at 2′,3′-positions is well tolerated. Thus, compound **2a** has higher affinity for CB1 receptor and equal affinity for CB2 receptor when compared to the prototype (−)-Δ^8-THC. Importantly, introduction of (1′*R*)- or (1′*S*)-methyl substituents (analogues **2b**, **2c**) leads to substantial enhancement in CB1 and CB2 receptor affinities, an effect more accentuated in CB1 receptor (17- to 45-fold). This increase in the ligand's affinities for CB1 and CB2 receptors holds true when a second methyl group is added at the 1′-position (analogue **2d**). Likewise, transformation of the *gem*-dimethyl substitution into the bulkier but sterically more confined cyclobutyl ring maintains low nanomolar affinities for both receptors (analogue **2e**).

The rat,[38] mouse,[39] and human CB1 (hCB1) receptors[40] have 97−99% sequence identity across species and are not expected to exhibit variations in their K_i values. However, mouse CB2 receptor[41,42] (mCB2) exhibits only 82% sequence identity with the human clone[3] (hCB2). This divergent nature of mCB2 and hCB2 receptors could possibly result in species-based differences in affinity.[43,44] For this reason, the side chain ester analogues **2a−e** were also assayed using membranes from HEK293 cells expressing hCB2 receptors, and the results are listed in Table 1. We observe that the tested compounds exhibit similar binding affinities for both mouse and human CB2 receptors.

Overall, our binding data show that addition of methyl, *gem*-dimethyl, or cyclobutyl substituents at the 1′-position of the ester group containing side chain results in analogues with

dx.doi.org/10.1021/jm4016075 | J. Med. Chem. XXXX, XXX, XXX−XXX

Table 1. Affinities (K_i) of (−)-Δ^8-THC Ester/Acid Analogues for CB1 and CB2 Cannabinoid Receptors (95% Confidence Limits) and Their Half-Lives ($t_{1/2}$) for Plasma Esterases[d]

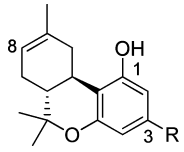

compd	R	(Ki, nM)[a]			mouse plasma	rat plasma
		rCB1	mCB2	hCB2	$t_{1/2}$ (min)[c]	$t_{1/2}$ (min)[c]
(-)-Δ^8-THC	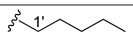	47.6[b]	39.3[b]	N D	N D	N D
2a	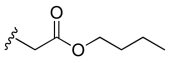	27.1 ± 4.5	40.4 ± 7.6	51.5 ± 11.2	0.7	< 0.5
3a	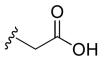	>10,000	>10,000	N D	N D	N D
2b	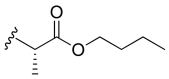	1.6 ± 0.2	4.5 ± 0.3	3.7 ± 0.2	5.9	10.5
3b	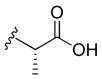	>10,000	>10,000	N D	N D	N D
2c	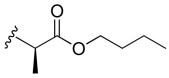	0.6 ± 0.2	6.2 ± 1.1	6.3 ± 1.2	4.0	4.3
3c	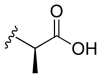	>10,000	>10,000	N D	N D	N D
2d	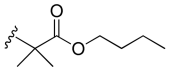	0.3 ± 0.1	2.1 ± 1.1	1.7 ± 0.4	12.4	120
3d	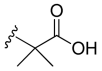	>10,000	>10,000	N D	N D	N D
2e	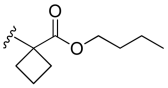	0.7 ± 0.2	3.0 ± 0.5	3.0 ± 0.7	36.3	263
3e	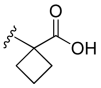	>10,000	>10,000	N D	N D	N D

[a]Affinities for CB1 and CB2 receptors were determined using rat brain (CB1) or membranes from HEK293 cells expressing mouse or human CB2 receptors and [^{3}H]CP-55,940 as the radioligand following previously described procedures.[23,26,62] Data were analyzed using nonlinear regression analysis. K_i values were obtained from three independent experiments run in duplicate and are expressed as the mean of the three values. [b]Reported previously.[21] [c]Half-lives ($t_{1/2}$) for mouse and rat plasma were determined as described in Experimental Section. [d]ND: not determined.

remarkably high affinities for both CB1 and CB2 receptors. All C1′ substituents lead to 20- to 50-fold enhancement in CB1 and CB2 receptor affinities, although the disubstituted analogues have 3- to 5-fold higher affinities than their respective monosubstituted counterparts. Also, the (1′*S*)-methyl analogue (**2c**) has a slightly higher affinity for CB1 receptor when compared to its (1′*R*)-diastereomer (**2b**).

Within the group of compounds reported here, this increase in CB receptor affinities is not significantly affected by the absolute stereochemistry and the size of the 1′-substituent. It is worthy to note that these side chain SAR trends parallel those we reported earlier for 1′-substituted tetrahydro-/hexahydrocannabinols and are congruent with the postulated presence of a subsite within the CB1 and CB2 receptor binding domain at the level of the benzylic side chain carbon.[21,23−26,45]

In Vitro Plasma Stability Studies. All ester carrying analogues were also assessed for their in vitro plasma stability toward mouse and rat plasma esterases as detailed in Experimental Section.[46,47] Examination of the half-lives ($t_{1/2}$) of **2a−e** (Table 1) shows that their mouse and rat plasma esterase stabilities correlate well with the presence and the size of the 1′-substituents, while the absolute configuration at the C1′ position has minimal effect on plasma stability. Thus, the order of metabolic stabilities is **2a** < **2c** ≤ **2b** < **2d** < **2e** with the compound carrying the bulkiest cyclobutyl group being the most stable. A comparison of the compounds' half-lives using

dx.doi.org/10.1021/jm4016075 | J. Med. Chem. XXXX, XXX, XXX−XXX

mouse and rat plasma indicates some species differences with the compounds carrying the bulkier 1′-substituents (**2d**, **2e**) exhibiting higher stability in rat plasma (7- to 10-fold) compared to mouse plasma. Also, in rat plasma the (1′*R*)-methyl analogue (**2b**) is somewhat more stable than the (1′*S*)-methyl counterpart (**2c**). Collectively, our data support the hypothesis that the duration of action of the 2′-ester analogues of Δ^8-THC can be strategically modulated by steric factors introduced by 1′-substituents.

Functional Characterization. Since the long-term goals of this project were aimed at developing compounds with analgesic activity, we focused on studying the functional properties of our analogues on CB1 receptor. For the side chain ester analogues **2a**–**e** for CB1 receptor these were obtained from adenylyl cyclase assays by measuring the decrease in forskolin-stimulated cAMP, as described in Experimental Section.[26] The respective EC_{50} values are listed in Table 2. We observe that compounds **2c**, **2d**, and **2e** are

Table 2. Functional Potencies (EC_{50}) of the (−)-Δ^8-THC Ester Analogues 2a–e for the rCB1 Cannabinoid Receptor

compd	rCB1 EC_{50} (nM)[a]	$E_{(max)}$ (%)[b]
2a	NR[c]	
2b	NR[c]	
2c	4.2 (1.7–10.9)	63
2d	0.5 (0.1–1.2)	92
2e	0.4 (0.2–1.2)	90

[a]Functional potencies at rCB1 receptor were determined by measuring the decrease in forskolin-stimulated cAMP levels, as described in Experimental Section.[26] EC_{50} values were calculated using nonlinear regression analysis. Data are the average of two independent experiments run in triplicate, and 95% confidence intervals for the EC_{50} values are given in parentheses. [b]Forskolin stimulated cAMP levels were normalized to 100%, and $E_{(max)}$ is the maximum inhibition of forskolin stimulated cAMP levels and is presented as the percentage of CP-55,940 response at 500 nM. [c]NR: no response up a 5 μM.

potent agonists at the CB1 receptor while their EC_{50} values correlate well with their respective binding affinities (Table 2). In contrast, compounds **2a** and **2b** show no response up to 5 μM. It is worthy to note that although both diastereomers **2b** and **2c** bind equally well at CB1 receptor, only **2c** exhibits significant CB1 receptor efficacy. This difference in the functional properties of the two diastereomers (**2b**, **2c**) reflects the effect of stereochemistry at the 1′-position which plays a major role in determining the ability of the ligand to activate the CB1 receptor notwithstanding the fact that both isomers exhibit similar affinities for the receptor.

In Vivo Behavioral Characterization. *Hypothermia Testing.* We determined the in vivo activity of the Δ^8-THC ester analogues, **2a**, **2b**, **2c**, **2d**, and **2e**, by assessing their effects on body temperature while the respective hydrolytic metabolites **3a**, **3b**, **3c**, **3d**, and **3e** had no hypothermic effects. Body temperature was measured in isolated rats over a 6 h period following drug injection (detailed procedures are given in Experimental Section). In agreement with our in vitro functional characterization, compounds **2a** and **2b** had no significant effects on body temperature, whereas **2c**, **2d**, and **2e** all decreased core body temperature in a dose-dependent manner, reducing body temperature by 3.6–4.8 °C at the highest doses tested (Figure 4). For comparison, effects of the nonhydrolyzable parent compound (−)-Δ^8-THC-DMH are

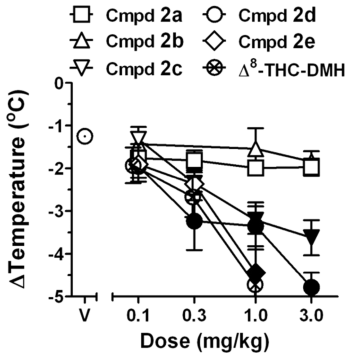

Figure 4. Effects of **2a**, **2b**, **2c**, **2d**, and **2e**, Δ^8-THC-DMH, or vehicle (above V) on body temperature: abscissa, dose, in mg/kg; ordinate, change in body temperature from an average baseline of 38.3 ± 0.3 °C. Symbols represent the average (±SEM; n = 6) of individual peak effects measured within 6 h of injection. Actual time varied with dose and compound. Solid symbols indicate effects that are significantly different from vehicle. (6a*R*,10a*R*)-3-(1,1-Dimethylheptyl)-6a,7,10,10a-tetrahydro-6,6,9-trimethyl-6*H*-dibenzo[*b*,*d*]pyran-1-ol (Δ^8-THC-DMH) was synthesized from commercially available (+)-*cis*/*trans*-*p*-mentha-2,8-dien-1ol and 3-(1,1-dimethylheptyl)-resorcinol in two steps according to procedures that we reported earlier for closely related analogues.[23,24]

also shown. Compounds **2c** and **2d** significantly reduced temperature at doses equal to or greater than 0.3 mg/kg, while **2e** induced hypothermia at 1.0 mg/kg. Compounds **2c**, **2d**, and **2e** all had maximum effects equivalent to those of Δ^8-THC-DMH ($F_{(3,19)}$ = 1.51, p > 0.05), and compound **2c** was slightly less potent than Δ^8-THC-DMH. The time course of the effects of the highest doses of **2a**, **2b**, **2c**, **2d**, and **2e** are shown in Figure 5. As evident in the dose effect functions, **2a** and **2b** had

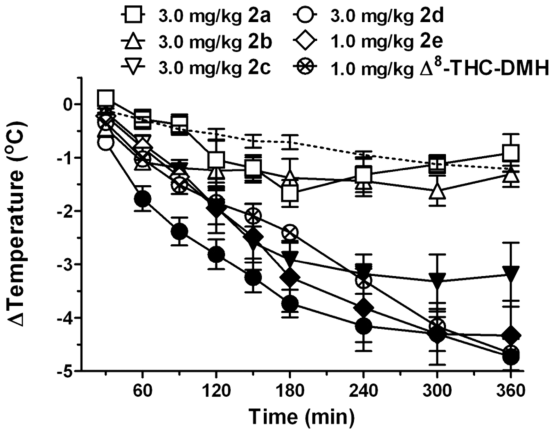

Figure 5. Hypothermic effects of the highest doses tested (3 mg/kg **2a**, **2b**, **2c**, **2d** and 1 mg/kg **2e** or Δ^8-THC-DMH) at different times after injection. The dotted line represents temperature changes after vehicle injection: abscissa, time (in min) after injection; ordinate, change in body temperature. Filled symbols indicate effects that are significantly different from vehicle.

no effect on body temperature (relative to vehicle effects) at any point over the course of the 6 h test. In contrast, **2c**, **2d**, and **2e** all reduced body temperature significantly for several hours after injection. Analogue **2d** had the fastest onset of drug effect, as significant effects were apparent within 60 min after injection whereas significant effects of **2c** and **2e** occurred at 90–120 min after injection. For all three Δ^8-THC ester

dx.doi.org/10.1021/jm4016075 | J. Med. Chem. XXXX, XXX, XXX–XXX

analogues, peak effects of the high doses were not reached until at least 300 min after injection. A comparison of the hypothermia induced by the ester drug **2d** and its nonhydrolyzable parent compound Δ^8-THC-DMH for a longer time frame using lower but equivalent doses revealed that the effects of 0.3 mg/kg compound **2d** reduced temperature by 2 °C within 2 h of injection and these effects were maintained up to 6 h after injection, after which there was a slow recovery toward baseline (Figure 6). In contrast, 0.3 mg/kg Δ^8-THC-DMH did not reduce temperature by 2 °C until 4 h after injection, and temperature was still reduced at 12 h after injection (Figure 6).

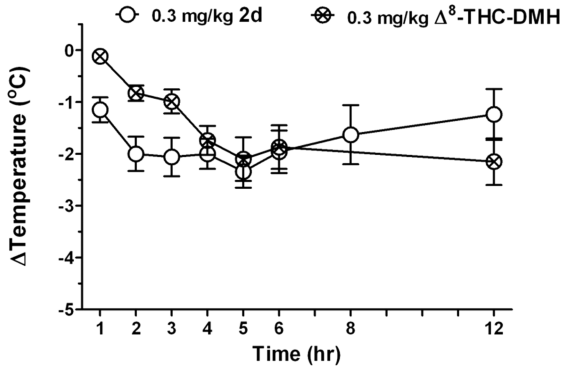

Figure 6. Hypothermic effects of the 0.3 mg/kg **2d** and Δ^8-THC-DMH at different times after injection: abscissa, time after injection; ordinate, change in body temperature.

Analgesia Testing. To confirm the observed pharmacokinetic differences between the ester analogue **2d** and its nonhydrolyzable congener, we used the CB1 receptor-characteristic analgesia test. Tail-flick latency data in mice involving compound **2d** and Δ^8-THC-DMH showed significant effects for dose (D) [$F_{(2,120)} = 160.6$; $P < 0.0001$] and time (T) [$F_{(7,120)} = 20.1$; $P < 0.0001$] as well as the $D \times T$ interaction [$F_{(14,120)} = 4.5$; $P < 0.0001$] involving three doses (0.1, 0.3, and 1.0 mg/kg) for each compound. The results are represented in Figure 7 which clearly demonstrate the faster onset and offset for **2d** when compared to Δ^8-THC-DMH. Note that the ANOVA did not include the vehicle group. The average (±SEM) baseline tail-flick withdrawal latency for all mice (N = 43) was 1.08 ± 0.08 s.

Our in vivo experiments show that compounds **2c**, **2d**, and **2e** have in vivo hypothermia activity and that they were able to produce similar maximum effects as other cannabinoid agonists.[26] The effects of all drugs, at the highest doses tested, lasted at least 6 h, and compound **2d** has a faster onset and shorter duration of action than Δ^8-THC-DMH for both the temperature and analgesia end points.

Molecular Modeling. We have used molecular modeling to refine our understanding with regard to binding affinity as well as enzymatic hydrolysis profiles of the synthesized compounds. Since among the analogues reported the only pharmacophoric variable is the side chain, we focused our attention on the conformational and stereoelectronic properties of this moiety. A conformational search of Δ^8-THC and the 2′-ester analogues **2a–e** in implicit water was carried out as described in the Experimental Section and the global energy minimum conformer for each compound was identified (see Supporting Information). As a representative example, the accessible conformational space for the side chain of the high affinity

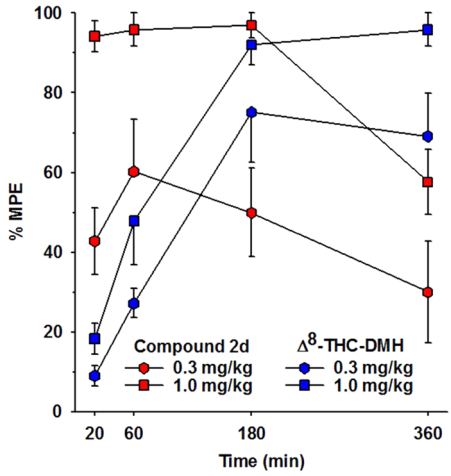

Figure 7. Tail-flick latencies in a hot water bath (52 °C) after administration of (−)-Δ^8-THC-DMH and its ester (compound **2d**) at four time-points (20, 60, 180, and 360 min after administration) using CD-1 mice: abscissa, time (min) after injection; ordinate, tail-flick withdrawal latencies expressed as a percentage of maximum possible effect (% MPE, group mean ± SEM). For clarity in data presentation, only the effects of the two higher doses of the two compounds are depicted in the graph. The average effects of 0.1 mg/kg of the two drugs and vehicle did not exceed 20% MPE at any of the four time-points examined.

and in vitro and in vivo potent CB1 receptor agonist **2e** is shown in Figure 8. The accessible conformational space for the *n*-pentyl substituent of Δ^8-THC is also included for comparison. Furthermore, the lowest energy conformers for all side chain ester analogues are depicted in Figure 9 where the van der Waals surface for the benzylic substituents is highlighted in yellow.

A comparison of the computational data points out the differences when the conformational spaces and the lowest energy conformers of Δ^8-THC and **2e** are compared (Figure 8) and may account for the different binding affinities of the two compounds. Our modeling shows that in the global minimum conformer of **2e** the butyl cyclobutanecarboxylate moiety adopts a "bent conformation" approximately perpendicular to the tricyclic system. In this conformation the 1′-cyclobutane ring can be well accommodated within a putative CB1 receptor subsite that we have postulated in our earlier work.[21,23−26,45] Since the conformation of the side chain for **2b**, **2c**, and **2d** is similar to that of **2e** (Figure 9), it can be argued that the smaller sized 1′-substituents of **2b**, **2c**, and **2d** can also fit within the subsite's groove and are congruent with the finding that all four 1′-substituted analogues have similar binding affinities. Conversely, the stabilities of the compounds for enzymatic hydrolysis are substantially different. The presence and size of 1′-substituents because of steric differences are expected to affect the ability of esterases to hydrolyze the ester bond. This is reflected in the stability half-lives of the compounds, with those carrying the bulkier substituents being more resistant to hydrolysis. This effect correlates well with the van der Waals surfaces of the 1′-substituents as represented by the yellow contours in Figure 9.

■ CONCLUSIONS

As a part of our program aimed at developing novel cannabinoids with controllable deactivation and improved druggability, we report here a series of (−)-Δ^8-THC analogues

dx.doi.org/10.1021/jm4016075 | J. Med. Chem. XXXX, XXX, XXX−XXX

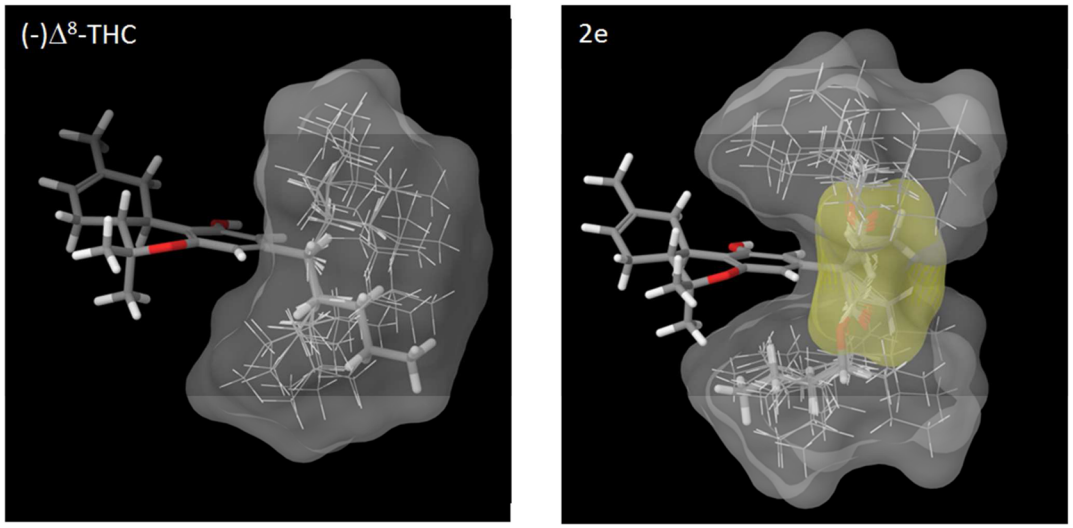

Figure 8. Accessible conformational space for the *n*-pentyl and butyl cyclobutanecarboxylate moieties of Δ^8-THC (left) and **2e** (right) using an energy window of 5 kcal mol^{-1}. The minimum energy conformers are shown in stick representation, while the van der Waals surface for the 1′-cyclobutane ring is shown in yellow.

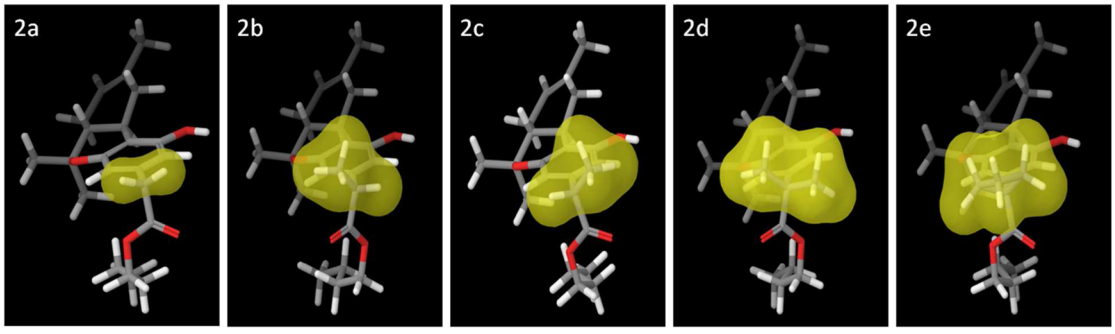

Figure 9. Lowest energy conformers for the Δ^8-THC ester analogues **2a–e**. The van der Waals surface for the 1′-substituent is shown in yellow. For each conformer in this view, the aromatic ring has been turned perpendicular to the plane of the page with the C1′ substituent closest to the viewer and the B/C ring system furthest from the viewer.

that incorporate a metabolically vulnerable ester group at the 2′-position of the cannabinoid side chain. We introduced variations in the steric properties and absolute configuration of the 1′-substituents adjacent to the ester moiety with the aim of controlling stability of the analogues toward enzymatic hydrolysis while enhancing the compounds' affinities for the CB receptors.

The in vitro results were consistent with the general drug design rationale as follows: (1) 1′-Substituted analogues show remarkably high affinities for CB1 and CB2 receptors. (2) Analogues incorporating an ester group at the side chain are susceptible to enzymatic (hydrolytic) deactivation in a controllable manner while at the same time maintaining excellent affinity and efficacy profiles. Thus, the 1′-(*S*)-methyl, 1′-*gem*-dimethyl, and 1′-cyclobutyl analogues **2c**, **2d**, and **2e** were all found to be potent agonists at CB1 receptors. (3) The respective metabolites are inactive at both CB1 and CB2 receptors and thus eliminate the possibility of undesirable cannabinoid receptor related side effects.

Preliminary in vivo characterization showed that compounds **2c**, **2d**, and **2e** have hypothermic profiles in rats with maximal effects comparable to those of other potent cannabinoid agonists. In agreement with our controlled-deactivation design, in both the temperature and analgesia assays, the C1′ *gem*-dimethyl analogue **2d** has faster onset and shorter duration of action compared to hydrolytically stable all-carbon side chain counterpart Δ^8-THC-DMH. The structure–activity and the structure–stability relationship results of this unexplored structural motif are highlighted by molecular modeling.

Finally, we have observed large differences between the in vitro and in vivo half-lives of our individual compounds reported here. This can be clearly attributed to the "depot effects" associated with the in vivo pharmacokinetic profile of these analogues. This effect, which is generally observed with all hydrophobic cannabinoid ligands, reflects the ability of the compound to be sequestered in some tissue reservoir and subsequently slowly become available for receptor activation and hydrolytic deactivation. This "depot effect" can be modulated by modifying the hydrophobic features of individual compounds. Thus, the introduction of polar groups within a hydrophobic analogue will be expected to reduce this depot effect.

The results reported here support the concept of selective detoxification which can be modulated by the design of ester encompassing cannabinoid ligands that are subject to variable rates of enzymatic hydrolysis. In future work we shall report on how the half-lives of our selectively detoxified-cannabinoid ligands can be controlled by the joint modulation of their relative stabilities toward plasma esterases as well as through variation of their depot effects.

dx.doi.org/10.1021/jm4016075 | *J. Med. Chem.* XXXX, XXX, XXX–XXX

EXPERIMENTAL SECTION

Materials. All reagents and solvents were purchased from Aldrich Chemical Co., unless otherwise specified, and used without further purification. All anhydrous reactions were performed under a static argon atmosphere in flame-dried glassware using scrupulously dry solvents. Flash column chromatography employed silica gel 60 (230–400 mesh). All compounds were demonstrated to be homogeneous by analytical TLC on precoated silica gel TLC plates (Merck, 60 F_{245} on glass, layer thickness 250 μm), and chromatograms were visualized by phosphomolybdic acid staining. Melting points were determined on a micromelting point apparatus and are uncorrected. IR spectra were recorded on a Perkin-Elmer Spectrum One FT-IR spectrometer. NMR spectra were recorded in $CDCl_3$, unless otherwise stated, on a Bruker Ultra Shield 400 WB Plus (^{1}H at 400 MHz, ^{13}C at 100 MHz) or on a Varian INOVA-500 (^{1}H at 500 MHz, ^{13}C at 125 MHz) spectrometer, and chemical shifts are reported in units of δ relative to internal TMS. Multiplicities are indicated as br (broadened), s (singlet), d (doublet), t (triplet), q (quartet), m (multiplet), and coupling constants (J) are reported in hertz (Hz). Low- and high-resolution mass spectra were performed in School of Chemical Sciences, University of Illinois at Urbana—Champaign. Mass spectral data are reported in the form of m/z (intensity relative to base of 100). Results from elemental analyses were obtained from Baron Consulting Co., Milford, CT, and were within ±0.4% of the theoretical values (see Supporting Information). Purities of the tested compounds were determined by elemental analysis or by HPLC (using Waters Alliance HPLC system, 4.6 mm × 250 mm, Supelco Discovery column, acetonitrile/water) and were >95%.

2-(3,5-Dimethoxyphenyl)acetic Acid (5).[48] A stirred mixture of (3,5-dimethoxyphenyl)acetonitrile (**4**, 5.7 g, 32.2 mmol) and NaOH (3.2 g, 80 mmol) in *n*-butanol/water (5 mL, 2:1 ratio) was refluxed for 4 h under argon. Volatiles were removed under reduced pressure, and the residue was acidified with 2 N HCl and diluted with diethyl ether. The organic layer was separated, and the aqueous layer was extracted with diethyl ether. The combined organic layer was washed with water and brine, dried ($MgSO_4$), and concentrated in vacuo. Purification by flash column chromatography on silica gel (30% ethyl acetate in hexane) gave **5** (5.61 g, 89% yield) as a white solid, mp 99–101 °C (lit.[48] 98–102 °C). IR (neat) 1695 (s, >C═O) cm^{-1}; ^{1}H NMR (500 MHz, $CDCl_3$) δ 6.43 (d, J = 2.3 Hz, 2H, ArH), 6.38 (t, J = 2.3 Hz, 1H, ArH), 3.77 (s, 6H, OMe), 3.57 (s, 2H, benzylic).

2-(3,5-Dihydroxyphenyl)acetic Acid (6).[49] To a stirred solution of **5** (3.5 g, 17.8 mmol) in dry CH_2Cl_2 (85 mL) at −78 °C, under an argon atmosphere, was added boron tribromide (62.3 mL, 62.3 mmol, 1 M solution in CH_2Cl_2). Following this addition, the reaction temperature was gradually raised over a period of 3 h to 25 °C, and the stirring was continued at that temperature until the reaction was completed (4 h). Unreacted boron tribromide was destroyed by the addition of methanol and ice at 0 °C. The resulting mixture was warmed to room temperature, and volatiles were removed in vacuo. The residue was dissolved in ethyl acetate and washed with water and brine and dried ($MgSO_4$). Solvent evaporation and purification by flash column chromatography on silica gel (40% ethyl acetate in hexane) gave **6** (2.64 g, 88% yield) as a white solid, mp 127–128 °C (lit.[49] 128–128.5 °C). IR (neat) 1697 (s, >C═O) cm^{-1}; ^{1}H NMR (500 MHz, CD_3OD) δ 6.21 (d, J = 2.0 Hz, 2H, ArH), 6.18 (t, J = 2.0 Hz, 1H, ArH), 3.4 (s, 2H, benzylic); mass spectrum (ESI) m/z (relative intensity) 169 (M^+ + H, 100), 123 (42).

2-[(6a*R*,10a*R*)-6a,7,10,10a-Tetrahydro-1-hydroxy-6,6,9-trimethyl-6*H*-dibenzo[*b*,*d*]pyran-3-yl]acetic Acid (3a).[50] To a stirred solution of **6** (1.0 g, 5.94 mmol) and (+)-*cis*/*trans*-*p*-mentha-2,8-dien-1-ol (1.0 g, 6.57 mmol) in anhydrous $CHCl_3$ (20 mL) under an argon atmosphere was added *p*-toluenesulfonic acid (230 mg, 1.21 mmol). The reaction mixture was refluxed for 6 h, and then it was cooled to room temperature and diluted with water and $CHCl_3$. The organic layer was separated, and the aqueous phase was extracted with $CHCl_3$. The combined organic layer was washed with water and brine and dried ($MgSO_4$). Solvent evaporation and purification by flash column chromatography on silica gel (20% ethyl acetate in hexane) gave **3a** (719 mg, 40% yield) as a light yellow gum. ^{1}H NMR (500 MHz, $CDCl_3$) δ 6.33 (d, J = 1.5 Hz, 1H, 4-H), 6.18 (d, J = 1.5 Hz, 1H, 2-H), 5.41 (m as d, J = 3.5 Hz, 1H, 8-H), 3.44 (s, 2H, 1′-H), 3.19 (dd, J = 16.0 Hz, J = 4.5 Hz, 1H, 10α-H), 2.67 (td, J = 11.0 Hz, J = 4.5 Hz, 1H, 10a-H), 2.18–2.08 (m, 1H, 7α-H), 1.85–1.73 (m, 3H, 10β-H, 7β-H, 6a-H), 1.67 (s, 3H, 9-CH_3), 1.36 (s, 3H, 6β-CH_3), 1.06 (s, 3H, 6α-CH_3); mass spectrum (ESI) m/z (relative intensity) 303 (M^+ + H, 100), 257 (15); mass spectrum (EI) m/z (relative intensity) 302 (M^+, 82), 287 (18), 259 (46), 234 (22), 219 (100), 181 (17), 84 (79); exact mass (EI) calculated for $C_{18}H_{22}O_4$ (M^+), 302.1518; found 302.1522. HPLC (4.6 mm × 250 mm, Supelco Discovery column, acetonitrile/water) showed purity of 97.8% and retention time of 9.1 min for **3a**. Anal. ($C_{18}H_{22}O_4$) C, H.

2-[(6a*R*,10a*R*)-6a,7,10,10a-Tetrahydro-1-hydroxy-6,6,9-trimethyl-6*H*-dibenzo[*b*,*d*]pyran-3-yl]acetic Acid Butyl Ester (2a). A stirred mixture of **3a** (175 mg, 0.58 mmol), bromobutane (195 mg, 1.42 mmol), and sodium bicarbonate (72 mg, 0.86 mmol) in DMF (2 mL) was heated at 165 °C for 12 min using microwave irradiation. The reaction mixture was cooled to room temperature and diluted with water and ethyl acetate. The organic layer was separated, and the aqueous phase was extraced with ethyl acetate. The combined organic layer was washed with brine, dried ($MgSO_4$), and concentrated under reduced pressure. Purification by flash column chromatography on silica gel gave **2a** (127 mg, 61% yield) as a light yellow gum. IR (neat) 3412, 2961, 1712 (s, >C═O), 1622, 1583, 1430 cm^{-1}; ^{1}H NMR (500 MHz, $CDCl_3$) δ 6.33 (d, J = 1.3 Hz, 1H, 4-H), 6.25 (d, J = 1.3 Hz, 1H, 2-H), 5.42 (m as d, J = 5.0 Hz, 1H, 8-H), 5.40 (s, 1H, OH), 4.09 (t, J = 5.5 Hz, 2H, -OCH_2-), 3.45 (s, 2H, 1′-H), 3.18 (dd, J = 15.0 Hz, J = 4.5 Hz, 1H, 10α-H), 2.70 (td, J = 11.0 Hz, J = 4.5 Hz, 1H, 10a-H), 2.22–2.09 (m, 1H, 7α-H), 1.86–1.73 (m, 3H, 10β-H, 7β-H, 6a-H), 1.69 (s, 3H, 9-CH_3), 1.61 (quintet, J = 7.0 Hz, 2H, -CH_2- of the side chain), 1.37 (s, 3H, 6β-CH_3), 1.34 (quintet, J = 7.5 Hz, 2H, -CH_2- of the side chain), 1.09 (s, 3H, 6α-CH_3), 0.91 (t, J = 7.5 Hz, 3H, 7′-H); ^{13}C NMR (125 MHz, $CDCl_3$) δ 172.2 (>C═O), 155.4 (C-1 or C-5), 155.3 (C-5 or C-1), 135.0, 133.6, 119.5, 112.3, 111.4, 108.4, 76.5 (C-6), 65.1 (-OCH_2-), 45.0 (C-6a), 41.2, 36.0, 31.8, 30.8, 28.1, 27.7, 23.7, 19.3, 18.7, 13.9 (C-7′); mass spectrum (ESI) m/z (relative intensity) 359 (M^+ + H, 100), 257 (15); mass spectrum (EI) m/z (relative intensity) 358 (M^+, 69), 343 (M^+ − 15, 13), 315 (32), 290 (18), 275 (100), 257 (22), 237 (23), 213 (38); exact mass (EI) calculated for $C_{22}H_{30}O_4$ (M^+), 358.2144; found 358.2143. HPLC (4.6 mm × 250 mm, Supelco Discovery column, acetonitrile/water) showed purity of 98.3% and retention time of 13.4 min for **2a**.

2-(3,5-Dimethoxyphenyl)acetyl Chloride (8).[51] To a stirred solution of 2-(3,5-dimethoxyphenyl)acetic acid (**5**, 1.0 g, 5.1 mmol) in dry CH_2Cl_2 (40 mL) at room temperature under an argon atmosphere was added the $SOCl_2$-BTA reagent [4.2 mL (6.3 mmol) of a 1.5 M solution in CH_2Cl_2, which was prepared by dissolving 5.46 mL (0.075 mol) of $SOCl_2$ and 8.93 g (0.075 mol) of BTA in 50 mL of CH_2Cl_2]. Stirring was continued for 20 min and insoluble materials were filtered off. The filtrate was washed with 1 N HCl, water, and brine and dried ($MgSO_4$). Solvent evaporation under reduced pressure afforded the title compound (1.0 g, 92% yield) which was used in the next step without further purification. ^{1}H NMR (500 MHz, $CDCl_3$) δ 6.42 (d, J = 2.2 Hz, 2H, ArH), 6.35 (t, J = 2.2 Hz, 1H, ArH), 3.97 (s, 2H, benzylic), 3.76 (s, 6H, OMe).

(4*R*)-4-Benzyl-3-[2-(3,5-dimethoxyphenyl)acetyl]oxazolidin-2-one (9). To a stirred solution of (4*R*)-4-benzyloxazolidin-2-one (**13**, 740 mg, 4.18 mmol) in dry THF (10 mL) at −30 °C under an argon atmosphere was added *n*-BuLi (2.6 mL, 4.2 mmol, 1.6 M solution in hexane) dropwise. Stirring was continued at the same temperature for 30 min, and then a solution of **8** (900 mg, 4.19 mmol) in dry THF (5 mL) was added. Following this addition, the mixture was gradually warmed to room temperature and stirred for 4 h. The reaction mixture was quenched with 1 M aqueous $NaHSO_4$ and extracted with ethyl acetate. The organic layer was washed with water and brine, dried ($MgSO_4$), and concentrated in vacuo. Flash column chromatography on silica gel (20% acetone in hexane) gave **9** (984 mg, 66% yield) as a colorless viscous oil. ^{1}H NMR (500 MHz, $CDCl_3$) δ 7.29 (t, J = 7.0 Hz, 2H, 3-H, 5-H, *Ph*CH_2-), 7.26 (t, J = 7.0 Hz, 1H, 4-H, *Ph*CH_2-),

dx.doi.org/10.1021/jm4016075 | J. Med. Chem. XXXX, XXX, XXX–XXX

7.14 (t, J = 7.0 Hz, 2H, 2-H, 6-H, $PhCH_2$-), 6.51 (d, J = 2.0 Hz, 2H, 2-H, 6-H, $(MeO)_2Ph$-), 6.39 (t, J = 2.0 Hz, 1H, 4-H, $(MeO)_2Ph$-), 4.67 (dddd, J = 9.3 Hz, J = 7.7 Hz, J = 3.0 Hz, J = 3.0 Hz, 1H, $PhCH_2$-CH<), 4.28 (d, J = 15.5 Hz, 1H, -CH_2-C(O)-), 4.19 (d, J = 15.5 Hz, 1H, -CH_2-C(O)-), 4.17 (dd, J = 9.5 Hz, J = 7.2 Hz, 1H, -CH_2-OC(O)-), 4.15 (dd, J = 9.5 Hz, J = 3.0 Hz, 1H, -CH_2-OC(O)-), 3.77 (s, 6H, -OMe), 3.25 (dd, J = 14.0 Hz, J = 3.0 Hz, 1H, $PhCH_2$-), 2.76 (dd, J = 14.0 Hz, J = 9.3 Hz, 1H, $PhCH_2$-); mass spectrum (ESI) m/z (relative intensity) 356 (M^+ + H, 100); exact mass (EI) calculated for $C_{20}H_{21}NO_5$ (M^+), 355.1420; found 355.1426.

(4*R*)-4-Benzyl-3-[(2*R*)-2-(3,5-dimethoxyphenyl)propanoyl]-oxazolidin-2-one (10). To a solution of **9** (980 mg, 2.76 mmol) in dry THF (20 mL) at −78 °C under an argon atmosphere was added a solution of sodium bis(trimethylsilyl)amide (3.0 mL, 3.0 mmol, 1 M solution in THF) over a period of 5 min. After the mixture was stirred for 1 h at −78 °C, iodomethane (1.0 mL, 14 mmol) was added. The reaction mixture was stirred for 1 h at −78 °C and for 1 h at −30 °C and then quenched by the addition of acetic acid in diethyl ether. Solid materials were filtered off, and the filtrate was concentrated under reduced pressure. Purification by flash column chromatography on silica gel (15% ethyl acetate in hexane) afforded the title compound (642 mg, 63% yield) as a light yellow viscous oil. ^{1}H NMR (500 MHz, $CDCl_3$) δ 7.32 (t, J = 8.0 Hz, 2H, 3-H, 5-H, $PhCH_2$-), 7.26 (t, J = 8.0 Hz, 1H, 4-H, $PhCH_2$-), 7.21 (t, J = 8.0 Hz, 2H, 2-H, 6-H, $PhCH_2$-), 6.53 (d, J = 2.5 Hz, 2H, 2-H, 6-H, $(MeO)_2Ph$-), 6.35 (t, J = 2.5 Hz, 1H, 4-H, $(MeO)_2Ph$-), 5.07 (q, J = 6.5 Hz, 1H, $(MeO)_2$Ph-CH(Me)-), 4.59 (dddd, J = 9.5 Hz, J = 8.0 Hz, J = 3.0 Hz, J = 3.0 Hz, 1H, $PhCH_2$-CH<), 4.09 (dd, J = 9.5 Hz, J = 2.0 Hz, 1H, -CH_2-OC(O)-), 4.05 (dd, J = 9.5 Hz, J = 8.5 Hz, 1H, -CH_2-OC(O)-), 3.76 (s, 6H, -OMe), 3.32 (dd, J = 13.5 Hz, J = 3.0 Hz, 1H, $PhCH_2$-), 2.80 (dd, J = 13.5 Hz, J = 10.0 Hz, 1H, $PhCH_2$-), 1.54 (d, J = 6.5 Hz, 3H, $(MeO)_2$Ph-CH(CH_3)-); mass spectrum (ESI) m/z (relative intensity) 370 (M^+ + H, 100); exact mass (EI) calculated for $C_{21}H_{23}NO_5$ (M^+), 369.1576; found 369.1577.

(2*R*)-2-(3,5-Dimethoxyphenyl)propanoic Acid (11). A mixture of **10** (600 mg, 1.62 mmol) and lithium hydroxide (114 mg, 4.76 mmol) in THF (6 mL)/H_2O (6 mL) was stirred at 0 °C for 2 h under argon. The reaction mixture was warmed to room temperature, and volatiles were removed in vacuo. The residue was acidified (10% HCl) until pH 1 and extracted with CH_2Cl_2. The organic layer was washed with water and brine and dried ($MgSO_4$). Solvent evaporation and purification by flash column chromatography on silica gel (66% ethyl acetate in hexane) gave **11** (171 mg, 50% yield) as a colorless viscous oil. ^{1}H NMR (500 MHz, $CDCl_3$) δ 6.47 (d, J = 2.5 Hz, 2H, 2-H, 6-H, ArH), 6.37 (t, J = 2.5 Hz, 1H, 4-H), 3.77 (s, 6H, -OMe), 3.66 (q, J = 7.5 Hz, 1H, -CHCH$_3$-), 1.48 (d, J = 7.5 Hz, 3H, -CHCH_3-); mass spectrum (ESI) m/z (relative intensity) 210 (M^+ + H, 85), 165 (100), 154 (45); exact mass (EI) calculated for $C_{11}H_{14}O_4$ (M^+), 210.0892; found 210.0887.

(2*R*)-2-(3,5-Dihydroxyphenyl)propanoic Acid (12). The synthesis was carried out as described for **6** using **11** (165 mg, 0.78 mmol) and boron tribromide (2.7 mL, 2.7 mmol, 1 M solution in CH_2Cl_2) in dry CH_2Cl_2 (20 mL) and gave **12** (104 mg, 73% yield) as a semisolid material. ^{1}H NMR (500 MHz, CD_3OD) δ 6.29 (d, J = 2.0 Hz, 2H, 2-H, 6-H, ArH), 6.18 (t, J = 2.0 Hz, 1H, 4-H), 5.09 (br s, 2H, -OH), 3.53 (q, J = 7.0 Hz, 1H, -CHCH$_3$-), 1.38 (d, J = 7.0 Hz, 3H, -CHCH_3-); mass spectrum (ESI) m/z (relative intensity) 183 (M^+ + H, 100); exact mass (EI) calculated for $C_9H_{10}O_4$ (M^+), 182.0579; found 182.0588.

(2*R*)-2-[(6a*R*,10a*R*)-6a,7,10,10a-Tetrahydro-1-hydroxy-6,6,9-trimethyl-6*H*-dibenzo[*b*,*d*]pyran-3-yl]propanoic Acid (3b). The synthesis was carried out as described for **3a** using **12** (90 mg, 0.49 mmol), (+)-*cis*/*trans*-*p*-mentha-2,8-dien-1-ol (83 mg, 0.55 mmol), and *p*-TSA (19 mg, 0.1 mmol) in $CHCl_3$ (8 mL) and gave **3b** (63 mg, 40% yield) as a light yellow gum. ^{1}H NMR (500 MHz, $CDCl_3$) δ 6.38 (d, J = 1.5 Hz, 1H, 4-H), 6.24 (d, J = 1.5 Hz, 1H, 2-H), 5.41 (m as d, J = 3.5 Hz, 1H, 8-H), 3.54 (q, J = 7.0 Hz, 1H, 1′-H), 3.19 (dd, J = 16.0 Hz, J = 4.0 Hz, 1H, 10α-H), 2.68 (td, J = 11.0 Hz, J = 4.0 Hz, 1H, 10a-H), 2.18−2.08 (m, 1H, 7α-H), 1.88−1.73 (m, 3H, 10β-H, 7β-H, 6a-H), 1.67 (s, 3H, 9-CH_3), 1.43 (d, J = 7.0 Hz, 3H, C1′-CH_3), 1.37 (s, 3H, 6β-CH_3), 1.08 (s, 3H, 6α-CH_3); mass spectrum (ESI) m/z (relative intensity) 317 (M^+ + H, 100), 271 (11); mass spectrum (EI) m/z (relative intensity) 316 (M^+, 77), 301 (18), 273 (39), 248 (24), 233 (100), 227 (29), 195 (20), 84 (41); exact mass (EI) calculated for $C_{19}H_{24}O_4$ (M^+), 316.1675; found 316.1676. HPLC (4.6 mm × 250 mm, Supelco Discovery column, acetonitrile/water) showed purity of 97.3% and retention time of 4.8 min for **3b**. Anal. ($C_{19}H_{24}O_4$) C, H.

(2*R*)-2-[(6a*R*,10a*R*)-6a,7,10,10a-Tetrahydro-1-hydroxy-6,6,9-trimethyl-6*H*-dibenzo[*b*,*d*]pyran-3-yl]propanoic Acid Butyl Ester (2b). The synthesis was carried out as described for **2a** using **3b** (58 mg, 0.18 mmol), bromobutane (49 mg, 0.36 mmol), and sodium bicarbonate (19 mg, 0.23 mmol) in DMF (2 mL) and gave **2b** (46 mg, 67% yield) as a light yellow gum. IR (neat) 3392, 2961, 1708 (s, >C═O), 1621, 1583, 1429 cm^{-1}; ^{1}H NMR (500 MHz, $CDCl_3$) δ 6.36 (d, J = 1.5 Hz, 1H, 4-H), 6.28 (d, J = 1.5 Hz, 1H, 2-H), 5.42 (m as d, J = 4.5 Hz, 1H, 8-H), 5.39 (s, 1H, OH), 4.08 (m, 2H, -OCH_2-), 3.54 (qt, J = 7.5 Hz, J = 3.5 Hz, 1H, 1′-H), 3.20 (dd, J = 15.0 Hz, J = 5.0 Hz, 1H, 10α-H), 2.69 (td, J = 10.5 Hz, J = 5.0 Hz, 1H, 10a-H), 2.17−2.10 (m, 1H, 7α-H), 1.87−1.73 (m, 3H, 10β-H, 7β-H, 6a-H), 1.69 (s, 3H, 9-CH_3), 1.57 (quintet, J = 7.0 Hz, 2H, -CH_2- of the side chain), 1.44 (d, J = 7.5 Hz, 3H, -CH(CH_3)-), 1.37 (s, 3H, 6β-CH_3), 1.30 (quintet, J = 7.5 Hz, 2H, -CH_2- of the side chain), 1.09 (s, 3H, 6α-CH_3), 0.88 (t, J = 7.5 Hz, 3H, 7′-H); ^{13}C NMR (125 MHz, $CDCl_3$) δ 174.1 (>C═O), 155.3 (C-1 or C-5), 155.1 (C-5 or C-1), 140.1, 134.9, 119.1, 112.2, 109.9 (C-2 or C-4), 106.2 (C-4 or C-2), 77.1 (C-6), 65.1 (-OCH_2-), 45.3, 45.0, 35.8, 31.6, 30.6, 28.5, 27.7, 23.5, 19.0, 18.9, 18.5, 14.1 (C-7′); mass spectrum (ESI) m/z (relative intensity) 373 (M^+ + H, 100), 329 (43); mass spectrum (EI) m/z (relative intensity) 372 (M^+, 87), 357 (M^+ − 15, 15), 329 (32), 317 (12), 304 (20), 289 (100), 271 (23), 251 (19), 227 (23); exact mass (EI) calculated for $C_{23}H_{32}O_4$ (M^+), 372.2301; found 372.2304. HPLC (4.6 mm × 250 mm, Supelco Discovery column, acetonitrile/water) showed purity of 98.2% and retention time of 6.5 min for **2b**. Anal. ($C_{23}H_{32}O_4$) C, H.

2-(3,5-Dimethoxyphenyl)propanenitrile (14).[52] A solution of (3,5-dimethoxyphenyl)acetonitrile (**4**, 5.0 g, 28.2 mmol) and iodomethane (6.0 g, 42.3 mmol) in dry DMF (30 mL) was added at −78 °C to a stirred suspension of sodium hydride (1.4 g, 34 mmol, 60% dispersion in oil) in dry DMF (50 mL). The reaction temperature rose to 25 °C over a 15 min period, and stirring was continued for 2 h. The reaction mixture was quenched with saturated NH_4Cl solution and diluted with ethyl acetate. The organic layer was separated, and the aqueous layer was extracted with ethyl acetate. The combined organic layer was washed with water and brine, dried ($MgSO_4$), and concentrated in vacuo. Purification by flash column chromatography on silica gel (20% ethyl acetate in hexane) gave the title compound (4.0 g, 75% yield) as a colorless oil. IR (neat): 2940, 2242, 1595, 1151 cm^{-1}; ^{1}H NMR (500 MHz, $CDCl_3$) δ 6.54 (d, J = 2.5 Hz, 2H, 2-H, 6-H, ArH), 6.41 (t, J = 2.5 Hz, 1H, 4-H, ArH), 3.84 (q, J = 7.0 Hz, 1H, benzylic), 3.81 (s, 6H, -OMe), 1.63 (d, J = 7.0 Hz, 3H, C1′-CH_3); mass spectrum (ESI) m/z (relative intensity) 192 (M^+ + H, 100), 165 (M^+ − CN, 52).

2-(3,5-Dimethoxyphenyl)propanoic Acid (15).[52] The synthesis was carried out as described for **5** using **14** (2.3 g, 12.0 mmol) and sodium hydroxide (1.2 g, 30.0 mmol) in 3 mL of *n*-butanol/water (2:1 ratio) and gave **15** (2.3 g, 92% yield) as a colorless oil. Spectroscopic data were identical to those of the pure enantiomer **11**.

2-(3,5-Dihydroxyphenyl)propanoic Acid (16).[53] The synthesis was carried out as described for **6** using **15** (2.3 g, 10.9 mmol) and boron tribromide (38.4 mL, 38.4 mmol, 1 M solution in CH_2Cl_2) and in dry CH_2Cl_2 (30 mL) and gave **16** (1.55 g, 78% yield) as a semisolid material. Spectroscopic data were identical to those of the pure enantiomer **12**.

2-[(6a*R*,10a*R*)-6a,7,10,10a-Tetrahydro-1-hydroxy-6,6,9-trimethyl-6*H*-dibenzo[*b*,*d*]pyran-3-yl]propanoic Acid (17). The synthesis was carried out as described for **3a** using **16** (660 mg, 3.62 mmol), (+)-*cis*/*trans*-*p*-mentha-2,8-dien-1-ol (609 mg, 4.0 mmol), and *p*-TSA (138 mg, 0.73 mmol), in $CHCl_3$ (30 mL) and gave **17** as an equally populated mixture of diasteromers **3b** and **3c** (527 mg, 46% yield, yellow gum). ^{1}H NMR (500 MHz, $CDCl_3$) δ 6.38 (d, J = 1.5 Hz, 1H, 4-H of **3b**), 6.37 (d, J = 1.5 Hz, 1H, 4-H of **3c**), 6.24 (d and d

dx.doi.org/10.1021/jm4016075 | J. Med. Chem. XXXX, XXX, XXX−XXX

overlapping, 2H, 2-H of **3b** and **3c**), 5.41 (m as d, J = 3.5 Hz, 2H, 8-H of **3b** and **3c**), 3.54 (q, J = 7.0 Hz, 2H, 1′-H of **3b** and **3c**), 3.19 (dd, J = 16.0 Hz, J = 4.0 Hz, 2H, 10α-H of **3b** and **3c**), 2.68 (td, J = 11.0 Hz, J = 4.0 Hz, 2H, 10a-H of **3b** and **3c**), 2.18−2.08 (m, 2H, 7α-H of **3b** and **3c**), 1.88−1.73 (m, 6H, 10β-H, 7β-H, 6a-H of **3b** and **3c**), 1.67 (s, 6H, 9-CH_3 of **3b** and **3c**), 1.43 (d, J = 7.0 Hz, 3H, C1′-CH_3 of **3b**), 1.41 (d, J = 7.0 Hz, 3H, C1′-CH_3 of **3c**), 1.37 (s, 6H, 6β-CH_3 of **3b** and **3c**), 1.08 (s, 6H, 6α-CH_3 of **3b** and **3c**); mass spectrum (ESI) m/z (relative intensity) 317 (M^+ + H, 48), 271 (100).

2-[(6a*R*,10a*R*)-6a,7,10,10a-Tetrahydro-1-hydroxy-6,6,9-trimethyl-6*H*-dibenzo[*b*,*d*]pyran-3-yl]propanoic Acid Butyl Ester (18). The synthesis was carried out as described for **2a** using **17** (175 mg, 0.55 mmol), bromobutane (114 mg, 0.83 mmol), and sodium bicarbonate (55 mg 0.65 mmol) in DMF (2 mL) and gave **18** as an equally populated mixture of diasteromers **2b** and **2c** (146 mg, 71% yield, light yellow gum). IR (neat) 3398, 2961, 1732, 1708 (s, >C═O), 1182 cm^{-1}; ^1H NMR (500 MHz, $CDCl_3$) δ 6.36 (d, J = 1.5 Hz, 1H, 4-H of **2b**), 6.35 (d, J = 1.5 Hz, 1H, 4-H of **2c**), 6.30 (d and d overlapping, 2H, 2-H of **2b** and **2c**), 5.74 (s, 2H, OH of **2b** and **2c**), 5.42 (m as d, J = 4.5 Hz, 2H, 8-H of **2b** and **2c**), 4.08 (m, 4H, -OCH_2− of **2b** and **2c**), 3.54 (qt and qt overlapping, 2H, 1′-H of **2b** and **2c**), 3.20 (dd, J = 15.0 Hz, J = 5.0 Hz, 2H, 10α-H of **2b** and **2c**), 2.69 (td, J = 10.5 Hz, J = 5.0 Hz, 2H, 10a-H of **2b** and **2c**), 2.19−2.09 (m, 2H, 7α-H of **2b** and **2c**), 1.87−1.73 (m, 6H, 10β-H, 7β-H, 6a-H of **2b** and **2c**), 1.69 (s, 6H, 9-CH_3 of **2b** and **2c**), 1.57 (quintet, J = 7.0 Hz, 4H, -CH_2- of the side chain of **2b** and **2c**), 1.44 (d, J = 7.5 Hz, 3H, -CH(CH_3)- of **2b**), 1.42 (d, J = 7.5 Hz, 3H, -CH(CH_3)- of **2c**),1.37 (s, 6H, 6β-CH_3 of **2b** and **2c**), 1.30 (quintet, J = 7.5 Hz, 4H, -CH_2- of the side chain of **2b** and **2c**), 1.09 (s, 6H, 6α-CH_3 of **2b** and **2c**), 0.88 (t, J = 7.5 Hz, 3H, 7′-H of **2b**), 0.87 (t, J = 7.5 Hz, 3H, 7′-H of **2c**); mass spectrum (ESI) m/z (relative intensity) 373 (M^+ + H, 100), 329 (48).

(4*S*)-3-[2-(3,5-Dimethoxyphenyl)acetyl]-4-isopropyloxazolidin-2-one (19).[35] The synthesis was carried out as described for **9** using (*S*)-4-isopropyloxazolidin-2-one (**23**, 1.7 g, 13.2 mmol), *n*-BuLi (8.3 mL, 13.3 mmol, 1.6 M solution in hexane), and **8** (2.6 g, 12.1 mmol) in dry THF (45 mL) and gave **19** (2.4 g, 65% yield) as a colorless viscous oil. ^1H NMR (500 MHz, $CDCl_3$) δ 6.47 (d, J = 2.5 Hz, 2H, 2-H, 6-H, ArH), 6.37 (t, J = 2.5 Hz, 1H, 4-H, ArH), 4.43 (ddd, J = 8.5 Hz, J = 4.0 Hz, J = 3.5 Hz, 1H, >N-CH<), 4.29 (d, J = 14.5 Hz, 1H, -CH_2-C(O)-), 4.25 (d, J = 8.5 Hz, 1H, -CH_2OC(O)-), 4.20 (dd, J = 8.5 Hz, J = 3.5 Hz, 1H, -CH_2OC(O)-), 4.16 (d, J = 14.5 Hz, 1H, -CH_2-C(O)-), 3.77 (s, 6H, -OMe), 2.35 (septet of d, J = 7.0 Hz, J = 3.5 Hz, 1H, $(CH_3)_2CH$-), 0.88 (d, J = 7.0 Hz, 3H, $(CH_3)_2$CH-), 0.81 (d, J = 7.0 Hz, 3H, $(CH_3)_2$CH-); mass spectrum (ESI) m/z (relative intensity) 308 (M^+ + H, 28), 179 (100), 130 (10); exact mass (EI) calculated for $C_{16}H_{21}NO_5$ (M^+), 307.1420; found 307.1418.

(4*S*)-3-[(2*S*)-2-(3,5-Dimethoxyphenyl)propanoyl]-4-isopropyloxazolidin-2-one (20).[35] The synthesis was carried out as described for **10** using **19** (2.3 g, 7.48 mmol), sodium bis-(trimethylsilyl)amide (8.0 mL, 8.0 mmol, 1 M in THF), and iodomethane (2.35 mL, 37.7 mmol) in THF and gave **20** (1.97 g, 82% yield) as a colorless viscous oil. ^1H NMR (500 MHz, $CDCl_3$) δ 6.51 (d, J = 2.5 Hz, 2H, 2-H, 6-H, ArH), 6.34 (t, J = 2.5 Hz, 1H, 4-H, ArH), 5.10 (q, J = 7.0 Hz, 1H, $(MeO)_2$Ph-$CH(CH_3)$-), 4.36 (ddd, J = 8.5 Hz, J = 4.0 Hz, J = 3.5 Hz, 1H, >N-CH<), 4.15 (dd, J = 8.0 Hz, J = 3.5 Hz, 1H, -CH_2OC(O)-), 4.14 (d, J = 8.0 Hz, 1H, -CH_2OC(O)-), 3.76 (s, 6H, -OMe), 2.43 (septet of d, J = 7.0 Hz, J = 3.5 Hz, 1H, $(CH_3)_2CH$-), 1.49 (d, J = 7.0 Hz, 3H, $(MeO)_2$Ph-CH(CH_3)-), 0.92 (d, J = 7.0 Hz, 3H, $(CH_3)_2$CH-), 0.90 (d, J = 7.0 Hz, 3H, $(CH_3)_2$CH-); mass spectrum (ESI) m/z (relative intensity) 322 (M^+ + H, 98), 278 (100), 222 (27), 193 (77), 165 (63); exact mass (EI) calculated for $C_{17}H_{23}NO_5$ (M^+), 321.1576; found 321. 1579.

(2*S*)-2-(3,5-Dimethoxyphenyl)propanoic Acid (21).[35] The synthesis was carried out as described for **11** using **20** (1.90 g, 5.91 mmol) and lithium hydroxide (400 mg, 16.7 mmol) in THF (20 mL):H_2O (20 mL) and gave **21** (1.12 g, 90% yield). Spectroscopic and physical data were identical to those of the pure enantiomer **11**.

(2*S*)-2-(3,5-Dihydroxyphenyl)propanoic Acid (22). The synthesis was carried out as described for **6** using **21** (1.0 g, 4.76 mmol) and boron tribromide (16.0 mL, 16.0 mmol, 1 M solution in CH_2Cl_2) in dry CH_2Cl_2 (40 mL) and gave **22** (685 mg, 79% yield). Spectroscopic and physical data were identical to those of the pure enantiomer **12**.

(2*S*)-2-[(6a*R*,10a*R*)-6a,7,10,10a-Tetrahydro-1-hydroxy-6,6,9-trimethyl-6*H*-dibenzo[*b*,*d*]pyran-3-yl]propanoic Acid (3c). The synthesis was carried out as described for **3a** using **22** (250 mg, 1.37 mmol), (+)-*cis*/*trans*-*p*-mentha-2,8-dien-1-ol (230 mg, 1.51 mmol), and *p*-TSA (50 mg, 0.26 mmol), in refluxing $CHCl_3$ (4 h) and gave **3c** (178 mg, 41% yield) as a light yellow gum. ^1H NMR (500 MHz, $CDCl_3$) δ 6.37 (d, J = 1.5 Hz, 1H, 4-H), 6.24 (d, J = 1.5 Hz, 1H, 2-H), 5.41 (m as d, J = 3.5 Hz, 1H, 8-H), 3.54 (q, J = 7.0 Hz, 1H, 1′-H), 3.19 (dd, J = 16.0 Hz, J = 4.0 Hz, 1H, 10α-H), 2.68 (td, J = 11.0 Hz, J = 4.0 Hz, 1H, 10a-H), 2.18−2.08 (m, 1H, 7α-H), 1.88−1.73 (m, 3H, 10β-H, 7β-H, 6a-H), 1.67 (s, 3H, 9-CH_3), 1.41 (d, J = 7.0 Hz, 3H, C1′-CH_3), 1.37 (s, 3H, 6β-CH_3), 1.08 (s, 3H, 6α-CH_3); mass spectrum (ESI) m/z (relative intensity) 317 (M^+ + H, 100), 271 (19); mass spectrum (EI) m/z (relative intensity) 316 (M^+, 92), 301 (48), 248 (19), 233 (100), 227 (22), 195 (18); exact mass (EI) calculated for $C_{19}H_{24}O_4$ (M^+), 316.1675; found 316.1670. HPLC (4.6 mm × 250 mm, Supelco Discovery column, acetonitrile/water) showed purity of 97.4% and retention time of 9.2 min for **3c**. Anal. ($C_{19}H_{24}O_4$) C, H.

(2*S*)-2-[(6a*R*,10a*R*)-6a,7,10,10a-Tetrahydro-1-hydroxy-6,6,9-trimethyl-6*H*-dibenzo[*b*,*d*]pyran-3-yl]propanoic Acid Butyl Ester (2c). The synthesis was carried out as described for **2a** using **3c** (150 mg, 0.47 mmol), bromobutane (180 mg, 1.31 mmol), and sodium bicarbonate (60 mg, 0.71 mmol) in DMF and gave **2c** (111 mg, 63% yield) as a light yellow gum. IR (neat) 3406, 2962, 1707 (s, >C═O), 1621, 1583, 1429, 1182 cm^{-1}; ^1H NMR (500 MHz, $CDCl_3$) δ 6.35 (d, J = 1.5 Hz, 1H, 4-H), 6.28 (d, J = 1.5 Hz, 1H, 2-H), 5.42 (m as d, J = 4.5 Hz, 1H, 8-H), 5.24 (s, 1H, OH), 4.08 (m, 2H, -OCH_2-), 3.54 (qt, J = 7.5 Hz, J = 3.5 Hz, 1H, 1′-H), 3.20 (dd, J = 15.0 Hz, J = 5.0 Hz, 1H, 10α-H), 2.69 (td, J = 10.5 Hz, J = 5.0 Hz, 1H, 10a-H), 2.18−2.10 (m, 1H, 7α-H), 1.87−1.73 (m, 3H, 10β-H, 7β-H, 6a-H), 1.69 (s, 3H, 9-CH_3), 1.57 (quintet, J = 7.0 Hz, 2H, -CH_2- of the side chain), 1.42 (d, J = 7.5 Hz, 3H, -CH(CH_3)-), 1.37 (s, 3H, 6β-CH_3), 1.30 (quintet, J = 7.5 Hz, 2H, -CH_2- of the side chain), 1.09 (s, 3H, 6α-CH_3), 0.87 (t, J = 7.5 Hz, 3H, 7′-H); ^{13}C NMR (100 MHz, $CDCl_3$) δ 175.2 (>C═O), 155.5 (C-1 or C-5), 155.2 (C-5 or C-1), 140.2, 135.0, 119.2, 112.3, 109.8 (C-2 or C-4), 106.3 (C-4 or C-2), 77.0 (C-6), 65.0 (-OCH_2-), 45.3, 45.0, 36.0, 31.8, 30.8, 28.1, 27.8, 23.7, 19.3, 18.7, 18.5, 13.9 (C-7′); mass spectrum (EI) m/z (relative intensity) 372 (M^+, 100), 357 (M^+ − 15, 17), 329 (35), 304 (21), 289 (98), 271 (26), 251 (17), 227 (25); exact mass (EI) calculated for $C_{23}H_{32}O_4$ (M^+), 372.2301; found 372.2299. HPLC (4.6 mm × 250 mm, Supelco Discovery column, acetonitrile/water) showed purity of 97.3% and retention time of 13.4 min for **2c**. Anal. ($C_{23}H_{32}O_4$) C, H.

2-(3,5-Dimethoxyphenyl)-2-methylpropanenitrile (24a).[54] To a stirred suspension of sodium hydride (6.7 g, 169.0 mmol) in dry DMF (40 mL) at 0 °C under an argon atmosphere was added dropwise a solution of **4** (10.0 g, 56.4 mmol) and iodomethane (10.5 mL, 169.0 mmol) in dry DMF (40 mL). The reaction temperature rose to 25 °C over a 15 min period, and stirring was continued for 2 h. The reaction mixture was quenched with saturated aqueous NH_4Cl solution and diluted with diethyl ether. The organic layer was separated, and the aqueous layer was extracted with diethyl ether. The combined organic layer was washed with water and brine, dried ($MgSO_4$), and concentrated in vacuo. Purification by flash column chromatography on silica gel (25% ethyl acetate in hexane) gave the title compound (11.0 g, 95% yield) as a colorless oil. ^1H NMR (500 MHz, $CDCl_3$) δ 6.61 (d, J = 2.0 Hz, 2H, ArH), 6.40 (t, J = 2.0 Hz, 1 H, ArH), 3.81 (s, 6 H, -OCH_3), 1.71 (s, 6 H, -C(CH_3)$_2$-); mass spectrum (ESI) m/z (relative intensity) 206 (M^+ + H, 100).

1-(3,5-Dimethoxyphenyl)cyclobutanecarbonitrile (24b).[23,36] The synthetic procedure was reported previously, along with physical and spectral data.[23]

2-(3,5-Dimethoxyphenyl)-2-methylpropanoic Acid (25a).[54] The synthesis was carried out as described for **5** using **24a** (4.0 g, 19.5 mmol) and sodium hydroxide (1.9 g, 47.5 mmol) in 3 mL of *n*-butanol/water (2:1 ratio) and gave **25a** (4.0 g, 93% yield) as a white

dx.doi.org/10.1021/jm4016075 | J. Med. Chem. XXXX, XXX, XXX−XXX

solid, mp 97−99 °C (lit.[54] 99 °C). IR (neat) 2926, 1695 (>C═O), 1598, 1454, 1288, 1204, 1068 cm^{-1}; ^1H NMR (500 MHz, $CDCl_3$) δ 6.54 (d, J = 2.5 Hz, 2H, ArH), 6.37 (t, J = 2.5 Hz, 1 H, ArH), 3.79 (s, 6 H, -OCH_3), 1.57 (s, 6 H, -$C(CH_3)_2$-); mass spectrum (ESI) m/z (relative intensity) 225 (M^+ + H, 10), 190 (7), 179 (33), 149 (100).

1-(3,5-Dimethoxyphenyl)cyclobutanecarboxylic Acid (25b). The synthesis was carried out as described for **5** using **24b** (760 mg, 3.5 mmol) and sodium hydroxide (350 mg, 8.75 mmol) in aqueous *n*-butanol/water (2:1 ratio) and gave **25b** (727 mg, 88% yield) as a white solid, mp 70−71 °C. ^1H NMR (500 MHz, $CDCl_3$) δ 12.08 (br s, 1H, -COOH), 6.51 (d, J = 2.5 Hz, 2H, ArH), 6.40 (t, J = 2.5 Hz, 1 H, ArH), 3.79 (s, 6 H, -OCH_3), 2.90−2.80 (m, 2H of the cyclobutane ring), 2.56 (m as q, J = 9.0 Hz, 2H of the cyclobutane ring), 2.16−2.04 (m, 1H of the cyclobutane ring), 1.95−1.80 (m, 1H of the cyclobutane ring); mass spectrum (ESI) m/z (relative intensity) 236 (M^+ + H, 30), 191 (100); exact mass (ESI) calculated for $C_{13}H_{17}O_4$ (M^+ + 1), 237.1127; found 237.1121.

2-(3,5-Dihydroxyphenyl)-2-methylpropanoic Acid (26a). The synthesis was carried out as described for **6** using **25a** (3.0 g, 13.4 mmol) and boron tribromide (48.0 mL, 48.0 mmol, 1 M solution in CH_2Cl_2) in dry CH_2Cl_2 (80 mL) and gave **26a** (2.23 g, 85% yield) as a white solid, mp 174−176 °C. IR (neat) 3180, 1688, 1601 cm^{-1}; ^1H NMR (500 MHz, CD_3OD) δ 6.33 (d, J = 2.5 Hz, 2 H, ArH), 6.15 (t, J = 2.5 Hz, 1 H, ArH), 4.91 (br s, 2H, -OH), 1.48 (s, 6 H, -$C(CH_3)_2$-); mass spectrum (ESI) m/z (relative intensity) 197 (M^+ + H, 100); exact mass (ESI) calculated for $C_{10}H_{13}O_4$ (M^+ + 1), 197.0814; found 197.0806.

1-(3,5-Dihydroxyphenyl)cyclobutanecarboxylic Acid (26b). The synthesis was carried out as described for **6** using **25b** (700 mg, 2.96 mmol) and boron tribromide (11.8 mL, 11.8 mmol, 1.0 M solution in CH_2Cl_2) in dry CH_2Cl_2 and gave **26b** (537 mg, 87%) as a brown viscous oil. ^1H NMR (500 MHz, CD_3OD) δ 6.28 (d, J = 2.0 Hz, 2H, ArH), 6.15 (t, J = 2.0 Hz, 1 H, ArH), 2.78−2.70 (m, 2H of the cyclobutane ring), 2.49−2.40 (m, 2H of the cyclobutane ring), 2.22−1.93 (m, 1H of the cyclobutane ring), 1.90−1.80 (m, 1H of the cyclobutane ring); mass spectrum (ESI) m/z (relative intensity) 209 (M^+ + H, 17), 163 (100); exact mass (EI) calculated for $C_{11}H_{12}O_4$ (M^+), 208.0736; found 208.0730.

2-[(6a*R*,10a*R*)-6a,7,10,10a-Tetrahydro-1-hydroxy-6,6,9-trimethyl-6*H*-dibenzo[*b*,*d*]pyran-3-yl]-2-methylpropanoic Acid (3d). The synthesis was carried out as described for **3a** using **26a** (800 mg, 4.08 mmol), (+)-*cis*/*trans*-*p*-mentha-2,8-dien-1-ol (680 mg, 4.47 mmol), and *p*-TSA (150 mg, 0.79 mmol) in $CHCl_3$ (30 mL) and gave **3d** (526 mg, 39% yield) as a light yellow gum. IR (neat) 2971, 2920, 1699 cm^{-1}; ^1H NMR (500 MHz, $CDCl_3$) δ 6.45 (d, J = 2.0 Hz, 1H, 4-H), 6.29 (d, J = 2.0 Hz, 1H, 2-H), 5.42 (m as d, J = 3.5 Hz, 1H, 8-H), 3.21 (dd, J = 16.0 Hz, J = 4.0 Hz, 1H, 10α-H), 2.67 (td, J = 11.0 Hz, J = 4.0 Hz, 1H, 10a-H), 2.18−2.09 (m, 1H, 7α-H), 1.88−1.73 (m, 3H, 10β-H, 7β-H, 6a-H), 1.69 (s, 3H, 9-CH_3), 1.51 (s, 3H, 1′-CH_3), 1.49 (s, 3H, 1′-CH_3), 1.38 (s, 3H, 6β-CH_3), 1.09 (s, 3H, 6α-CH_3); mass spectrum (ESI) m/z (relative intensity) 331 (M^+ + H, 100), 285 (9); exact mass (ESI) calculated for $C_{20}H_{27}O_4$ (M^+ + 1), 331.1909; found 331.1901. HPLC (4.6 mm × 250 mm, Supelco Discovery column, acetonitrile/water) showed purity of 95.2% and retention time of 9.6 min for **3d**. Anal. ($C_{20}H_{26}O_4$) C, H.

1-[(6a*R*,10a*R*)-6a,7,10,10a-Tetrahydro-1-hydroxy-6,6,9-trimethyl-6*H*-dibenzo[*b*,*d*]pyran-3-yl]cyclobutanecarboxylic Acid (3e). The synthesis was carried out as described for **3a** using **26b** (500 mg, 2.4 mmol), (+)-*cis*/*trans*-*p*-mentha-2,8-dien-1-ol (400 mg, 2.63 mmol), and *p*-TSA (90 mg, 0.47 mmol) in $CHCl_3$ (12 mL) and gave **3e** (370 mg, 45% yield) as a light yellow gum. IR (neat) 2975, 2920, 1701 cm^{-1}; ^1H NMR (500 MHz, $CDCl_3$) δ 6.45 (d, J = 1.5 Hz, 1H, 4-H), 6.29 (d, J = 1.5 Hz, 1H, 2-H), 5.43 (m as d, J = 3.5 Hz, 1H, 8-H), 3.23 (dd, J = 16.0 Hz, J = 4.0 Hz, 1H, 10α-H), 2.78−2.68 (m, 3H, 10a-H, 2H of the cyclobutane ring, overlapping), 2.44 (m as sextet, J = 11.0 Hz, 2H of the cyclobutane ring), 2.18−2.10 (m, 1H, 7α-H), 2.25−1.92 (m, 1H of the cyclobutane ring), 1.88−1.75 (m, 4H, 10β-H, 7β-H, 6a-H and 1H of the cyclobutane ring overlapping), 1.70 (s, 3H, 9-CH_3), 1.39 (s, 3H, 6β-CH_3), 1.11 (s, 3H, 6α-CH_3); mass spectrum (ESI) m/z (relative intensity) 343 (M^+ + H, 100), 297 (13); exact mass (ESI) calculated for $C_{21}H_{27}O_4$ (M^+ + 1), 343.1909; found 343.1897. HPLC (4.6 mm × 250 mm, Supelco Discovery column, acetonitrile/water) showed purity of 95.8% and retention time of 4.8 min for **3e**. Anal. ($C_{21}H_{26}O_4$) C, H.

2-[(6a*R*,10a*R*)-6a,7,10,10a-Tetrahydro-1-hydroxy-6,6,9-trimethyl-6*H*-dibenzo[*b*,*d*]pyran-3-yl]-2-methylpropanoic Acid Butyl Ester (2d). The synthesis was carried out as described for **2a** using **3d** (325 mg, 0.98 mmol), bromobutane (130 mg, 0.95 mmol), and sodium bicarbonate (82 mg, 0.98 mmol) in DMF (2.5 mL) and gave **2d** (259 mg, 68% yield) as a light yellow gum. IR (neat) 3413, 2962, 2932, 1728 (s, >C═O), 1702 cm^{-1}; ^1H NMR (500 MHz, $CDCl_3$) δ 6.42 (d, J = 1.5 Hz, 1H, 4-H), 6.25 (d, J = 1.5 Hz, 1H, 2-H), 5.42 (m as d, J = 5.0 Hz, 1H, 8-H), 5.11 (s, 1H, OH), 4.09 (t, J = 6.5 Hz, 2H, -OCH_2-), 3.19 (dd, J = 15.0 Hz, J = 4.5 Hz, 1H, 10α-H), 2.69 (td, J = 11.0 Hz, J = 4.5 Hz, 1H, 10a-H), 2.18−2.10 (m, 1H, 7α-H), 1.86−1.74 (m, 3H, 10β-H, 7β-H, 6a-H), 1.70 (s, 3H, 9-CH_3), 1.55 (quintet, J = 7.0 Hz, 2H, -CH_2- of the side chain), 1.50 (s, 6H, -$C(CH_3)_2$-), 1.38 (s, 3H, 6β-CH_3), 1.26 (quintet, J = 7.5 Hz, 2H, -CH_2- of the side chain), 1.10 (s, 3H, 6α-CH_3), 0.86 (t, J = 7.5 Hz, 3H, 7′-H); ^{13}C NMR (125 MHz, $CDCl_3$) δ 172.1 (>C═O), 155.3 (C-1 or C-5), 154.9 (C-5 or C-1), 144.2, 135.1, 119.3, 112.1, 108.2, 105.5, 77.2 (C-6), 65.2 (-OCH_2-), 52.1, 44.8, 35.7, 32.0, 31.8, 31.3, 30.5, 28.7, 27.5, 23.5, 19.1, 18.5, 13.8 (C-7′); mass spectrum (ESI) m/z (relative intensity) 387 (M^+ + H, 100), 285 (32); mass spectrum (EI) m/z (relative intensity) 386 (M^+, 98), 371 (M^+ − 15, 12), 343 (31), 331 (7), 318 (9), 303 (100), 285 (65), 265 (20), 241 (35); exact mass (EI) calculated for $C_{24}H_{34}O_4$ (M^+), 386.2457; found 386.2460. HPLC (4.6 mm × 250 mm, Supelco Discovery column, acetonitrile/water) showed purity of 96.5% and retention time of 13.5 min for **2d**.

1-[(6a*R*,10a*R*)-6a,7,10,10a-Tetrahydro-1-hydroxy-6,6,9-trimethyl-6*H*-dibenzo[*b*,*d*]pyran-3-yl]cyclobutanecarboxylic Acid Butyl Ester (2e). The synthesis was carried out as described for **2a** using **3e** (90 mg, 0.26 mmol), bromobutane (89 mg, 0.65 mmol), and sodium bicarbonate (40 mg, 0.48 mmol) in DMF (1.5 mL) and gave **2e** (70 mg, 67% yield) as a light yellow gum. IR (neat) 3409, 2959, 1728, and 1702 (s, >C═O), 1620, 1578, 1278 cm^{-1}; ^1H NMR (500 MHz, $CDCl_3$) δ 6.39 (d, J = 2.0 Hz, 1H, 4-H), 6.27 (d, J = 2.0 Hz, 1H, 2-H), 6.10 (s, 1H, -OH), 5.42 (m as d, J = 3.5 Hz, 1H, 8-H), 4.07 (m, 2H, -OCH_2-), 3.23 (dd, J = 16.0 Hz, J = 4.0 Hz, 1H, 10α-H), 2.79−2.67 (m, 3H, 10a-H, 2H of the cyclobutane ring, overlapping), 2.45 (m as qt, J = 9.5 Hz, 2H of the cyclobutane ring), 2.18−2.10 (m, 1H, 7α-H), 1.99−1.90 (m, 1H of the cyclobutane ring), 1.88−1.74 (m, 4H, 10β-H, 7β-H, 6a-H and 1H of the cyclobutane ring overlapping), 1.69 (s, 3H, 9-CH_3), 1.54 (m as qt, J = 7.0 Hz, 2H, -CH_2- of the side chain), 1.38 (s, 3H, 6β-CH_3), 1.26 (m as qt, J = 7.5 Hz, 2H, -CH_2- of the side chain), 1.09 (s, 3H, 6α-CH_3), 0.85 (t, J = 7.5 Hz, 3H, 7′-H); ^{13}C NMR (100 MHz, $CDCl_3$) δ 167.5 (>C═O), 155.2 (C-1 or C-5), 154.8 (C-5 or C-1), 143.1, 134.8, 119.2, 111.6, 108.1 (C-2 or C-4), 105.4 (C-4 or C-2), 76.8 (C-6), 64.9 (-OCH_2-), 52.2 (C-1′), 44.8, 35.8, 32.7 (cyclobutane ring), 32.0 (cyclobutane ring), 31.6, 30.5, 28.9, 27.6, 23.5, 19.0, 18.5, 16.5, 13.7 (C-7′); mass spectrum (ESI) m/z (relative intensity) 399 (M^+ + H, 100); exact mass (ESI) calculated for $C_{25}H_{35}O_4$ (M^+ + 1), 399.2535; found 399.2536. HPLC (4.6 mm × 250 mm, Supelco Discovery column, acetonitrile/water) showed purity of 96.8% and retention time of 6.8 min for **2e**. Anal. ($C_{25}H_{34}O_4$) C, H.

Radioligand Binding Assays. *Rat brain CB1 Receptor and Mouse and Human CB2 Receptor Binding Assays.* Compounds were tested for their affinities for the CB1 and CB2 receptors using membrane preparations from rat brain or HEK293 cells expressing either mCB2 or hCB2 receptor, respectively, and [^{3}H]CP-55,940, as previously described.[23,24,26] Results from the competition assays were analyzed using nonlinear regression to determine the IC_{50} values for the ligand. K_i values were calculated from the IC_{50} [55] (Prism by GraphPad Software, Inc.). Each experiment was performed in duplicate, and K_i values were determined from three independent experiments and are expressed as the mean of the three values.

cAMP Assay.[26] HEK293 cells stably expressing rCB1 receptor were used for the studies. The cAMP assay was carried out using PerkinElmer's Lance ultra cAMP kit following the protocol of the

dx.doi.org/10.1021/jm4016075 | J. Med. Chem. XXXX, XXX, XXX−XXX

manufacturer. Briefly, the assays were carried out in 384-well plates using 1000−1500 cells/well. The cells were harvested with non-enzymatic cell dissociation reagent Versene and were washed once with HBSS and resuspended in the stimulation buffer. The various concentrations of the test compound (5 μL) in forskolin (2 μM final concentration) containing stimulation buffer were added to the plate followed by the cell suspension (5 μL). The cells were stimulated for 30 min at room temperature. Then Eu-cAMP tracer working solution (5 μL) and Ulight-anti-cAMP working solution (5 μL) were added to the plate and incubated at room temperature for 60 min. The data were collected on a Perkin-Elmer Envision instrument. The EC_{50} values were determined by nonlinear regression analysis using GraphPad Prism software (GraphPad Software, Inc., San Diego, CA).

Plasma Stability.[46,47] Compounds or their proposed products were diluted (200 μM) in mouse or rat plasma and incubated at 37 °C, 100 rpm. At various time points, samples were taken, diluted 1:4 in acetonitrile, and centrifuged to precipitate the proteins. The resulting supernatant was analyzed by HPLC.

HPLC Analysis. Chromatographic separation was achieved using a Supelco Discovery C18 (4.6 mm × 250 mm) column on a Waters Alliance HPLC system. Mobile phase consisted of acetonitrile (A) and a mixture of 60% water (acidified with 8.5% *o*-phosphoric acid) and 40% acetonitrile (B). Gradient elution started with 5% A, transitioning to 95% A over 10 min and holding for 5 min before returning to starting conditions. Run time was 15 min. The flow rate was 1 mL/min, and UV detection was used at each compound's maximal absorbance (204 and 230 nm).

Methods for Characterization of in Vivo Effects.[26,56] *Subjects.* For hypothermia testing, female Sprague−Dawley rats (n = 6/group), weighing between 250 and 350 g (Charles River, Wilmington MA) were used. Rats were tested repeatedly with at least 5 days intervening between drug sessions. Experiments occurred at approximately the same time (10:00 a.m. to 5:00 p.m.) during the light portion of the daily light/dark cycle. Outside experimental sessions, rats were pair housed (2/cage) in a climate controlled vivarium with unrestricted access to food and water. For tail-flick withdrawal (analgesia) testing, male CD-1 mice (n = 6/group except for the vehicle condition where n = 7), weighting between 30 and 35 g (Charles River, Wilmington MA), were used. Mice were housed 4/cage in a climate controlled vivarium with unrestricted access to food and water and acclimated to these conditions for at least a week before any experimental manipulations occurred. Analgesia testing took place between 11:00 a.m. and 7:00 p.m. Mice were used once.

Procedures. Temperature was recorded using a thermistor probe (model 401, Measurement Specialties, Inc., Dayton, OH) inserted to a depth of 6 cm and secured to the tail with micropore tape. Rats were minimally restrained and isolated in 38 cm × 50 cm × 10 cm plastic stalls. Temperature was read to the nearest 0.01 °C using a thermometer (model 4000A, Measurement Specialties, Inc.).

Two baseline temperature measures were recorded at 15 min intervals, and drugs were injected immediately after the second baseline was recorded. After injection, temperature was recorded every 30 min for 3 h and every hour thereafter for a total of 6 h. In some studies, temperature readings at later time points were obtained by inserting the probe 6 cm and holding it in place for at least 1 min before taking a reading. The change in temperature was determined for each rat by subtracting temperature readings from the average of the two baseline measures. Analgesia testing utilized a thermostatically controlled 2 L water bath commercially available from VWR International where the water temperature was set at 52 °C (±0.5 °C). The tail was immersed into the water at a depth of 2 cm and the withdrawal latency recorded by a commercially available stopwatch (Fisher Scientific), allowing measurements in seconds and $^1/_{100}$ s. Cut-off was set at 10 s to minimize the risk of tissue damage. A test session consisted of five recordings, the first of which constituted the baseline recording. Injections occurred immediately after the baseline recording, and the remaining recordings took place 20, 60, 180, and 360 min after administration. Prior to this testing, the animals had been accustomed to the procedure for three consecutive sessions where the water was held at room temperature. The tail-flick withdrawal latencies are expressed as a percentage of maximum possible effect (% MPE), according to the formula % MPE = [(test latency minus baseline latency) divided by (10 minus baseline latency)] times 100.

Drugs. For hypothermia testing, Δ^8-THC-DMH and compounds **2a**, **2b**, **2c**, **2d**, and **2e** were initially dissolved in a solution of 20% ethanol, 20% alkamuls, and 60% saline and were further diluted with saline. Injections were administered sc in a volume of 1.0 mL/kg. For tail-flick withdrawal (analgesia) testing, (−)-Δ^8-THC-DMH and compound **2d** were initially dissolved in 2% dimethyl sulfoxide, 4% Tween-80, and 4% propylene glycol before saline was slowly added just prior to the 10 mL/kg ip administration. All suspensions were freshly prepared for analgesia testing.

Data Analysis. Time−effect functions were analyzed using two-way repeated measures ANOVA procedures followed by Bonferroni's post hoc test for both the hypothermia and tail-flick latency data. Hypothermia dose−effect functions for compounds **2a**, **2b**, **2c**, **2d**, and **2e** were analyzed using one-way repeated measures ANOVA procedures followed by the Holm−Sidak multiple comparison t test. p was set at <0.05, and statistical analyses were performed using the software package GraphPad Prism 5.03 (GraphPad Software, San Diego, CA).

Molecular Modeling. Compounds Δ^8-THC, **2a−e** underwent torsional sampling using the MCMM (Monte Carlo multiple minimum) protocol[57,58] in MacroModel.[59] The conformational search was conducted using the OPLS_2005 force field[60] in a GB/SA water model[61] with an extended cutoff. An energy window of 21.0 kJ mol^{-1} (5 kcal mol^{-1}) was employed, and the redundant conformers were eliminated using a rmsd cutoff of 0.5 Å for all atoms.

■ ASSOCIATED CONTENT

Supporting Information

Elemental analysis results for compounds **3a−e**, **2b**, **2c**, and **2e** and accessible conformational space for the side chains of Δ^8-THC and **2a−e**. This material is available free of charge via the Internet at http://pubs.acs.org.

■ AUTHOR INFORMATION

Corresponding Authors

*S.P.N.: phone, +1-617-373-7620; fax, +1-617-373-7493; e-mail, s.nikas@neu.edu.

*A.M.: phone, +1-617-373-4200; fax, +1-617-373-7493; e-mail, a.makriyannis@neu.edu.

Present Address

§R.S.: Microconstants Inc., 10191 Caminito Volar, San Diego, CA 92126. E-mail: sharmarishi2004@yahoo.co.in.

Notes

The authors declare no competing financial interest.

■ ACKNOWLEDGMENTS

This work was supported by grants from the National Institute on Drug Abuse (Grants DA009158, DA007215, and DA09064).

■ ABBREVIATIONS USED

CB1, cannabinoid receptor 1; CB2, cannabinoid receptor 2; (−)-Δ^9-THC, (−)-Δ^9-tetrahydrocannabinol; CNS, central nervous system; PK/PD, pharmacokinetic/pharmacodynamic; SC, side chain; SAR, structure−activity relationship; HEK293, human embryonic kidney cell line; log P, logarithm of the octanol−water partition coefficient; PSA, polar surface area; NMR, nuclear magnetic resonance; HPLC, high-performance liquid chromatography

REFERENCES

(1) Mechoulam, R.; Hanus, L. A historical overview of chemical research on cannabinoids. *Chem. Phys. Lipids* **2000**, *108*, 1−13.

(2) Devane, W. A.; Dysarz, F. A., 3rd; Johnson, M. R.; Melvin, L. S.; Howlett, A. C. Determination and characterization of a cannabinoid receptor in rat brain. *Mol. Pharmacol.* **1988**, *34*, 605−613.

(3) Munro, S.; Thomas, K. L.; Abu-Shaar, M. Molecular characterization of a peripheral receptor for cannabinoids. *Nature* **1993**, *365*, 61−65.

(4) Pertwee, R. G. Pharmacology of cannabinoid CB1 and CB2 receptors. *Pharmacol. Ther.* **1997**, *74*, 129−180.

(5) Pavlopoulos, S.; Thakur, G. A.; Nikas, S. P.; Makriyannis, A. Cannabinoid receptors as therapeutic targets. *Curr. Pharm. Des.* **2006**, *12*, 1751−1769.

(6) Hwang, J.; Adamson, C.; Butler, D.; Janero, D. R.; Makriyannis, A.; Bahr, B. A. Enhancement of endocannabinoid signaling by fatty acid amide hydrolase inhibition: a neuroprotective therapeutic modality. *Life Sci.* **2010**, *86*, 615−623.

(7) Karst, M.; Wippermann, S.; Ahrens, J. Role of cannabinoids in the treatment of pain and (painful) spasticity. *Drugs* **2010**, *70*, 2409−2438.

(8) Lu, D.; Vemuri, V. K.; Duclos, R. I., Jr.; Makriyannis, A. The cannabinergic system as a target for anti-inflammatory therapies. *Curr. Top. Med. Chem.* **2006**, *6*, 1401−1426.

(9) Marco, E. M.; Romero-Zerbo, S. Y.; Viveros, M. P.; Bermudez-Silva, F. J. The role of the endocannabinoid system in eating disorders: pharmacological implications. *Behav. Pharmacol.* **2012**, *23*, 526−536.

(10) Pertwee, R. G. Cannabinoid receptors and pain. *Prog. Neurobiol.* **2001**, *63*, 569−611.

(11) Jarvinen, T.; Pate, D. W.; Laine, K. Cannabinoids in the treatment of glaucoma. *Pharmacol. Ther.* **2002**, *95*, 203−220.

(12) Buchwald, A.; Derendorf, H.; Ji, F.; Nagaraja, N. Y.; Wu, W. M.; Bodor, N. Soft cannabinoid analogues as potential anti-glaucoma agents. *Pharmazie* **2002**, *57*, 108−114.

(13) Grotenhermen, F. Pharmacokinetics and pharmacodynamics of cannabinoids. *Clin. Pharmacokinet.* **2003**, *42*, 327−360.

(14) Karschner, E. L.; Darwin, W. D.; McMahon, R. P.; Liu, F.; Wright, S.; Goodwin, R. S.; Huestis, M. A. Subjective and physiological effects after controlled Sativex and oral THC administration. *Clin. Pharmacol. Ther.* **2011**, *89*, 400−407.

(15) Nikas, S. P.; Thakur, G. A.; Parrish, D.; Alapafuja, S. O.; Huestis, M. A.; Makriyannis, A. A concise methodology for the synthesis of (−)-Delta(9)-tetrahydrocannabinol and (−)-Delta(9)-tetrahydrocannabivarin metabolites and their regiospecifically deuterated analogs. *Tetrahedron* **2007**, *63*, 8112−8123.

(16) Bodor, N.; Buchwald, P. Soft drug design: general principles and recent applications. *Med. Res. Rev.* **2000**, *20*, 58−101.

(17) Bodor, N.; Buchwald, P. Ophthalmic drug design based on the metabolic activity of the eye: soft drugs and chemical delivery systems. *AAPS J.* **2005**, *7*, E820−E833.

(18) Bodor, N.; Buchwald, P. Recent advances in retrometabolic drug design (RMDD) and development. *Pharmazie* **2010**, *65*, 395−403.

(19) Minutolo, F.; Cascio, M. G.; Carboni, I.; Bisogno, T.; Prota, G.; Bertini, S.; Digiacomo, M.; Bifulco, M.; Di Marzo, V.; Macchia, M. Metabolically labile cannabinoid esters: a "soft drug" approach for the development of cannabinoid-based therapeutic drugs. *Bioorg. Med. Chem. Lett.* **2007**, *17*, 4878−4881.

(20) Buchwald, A.; Browne, C. E.; Wu, W. M.; Ji, F.; Bodor, N. Soft cannabinoid analogues as potential anti-glaucoma agents. *Pharmazie* **2000**, *55*, 196−201.

(21) Thakur, G. A.; Nikas, S. P.; Li, C.; Makriyannis, A. Structural requirements for cannabinoid receptor probes. *Handb. Exp. Pharmacol.* **2005**, 209−246.

(22) Thakur, G. A.; Nikas, S. P.; Makriyannis, A. CB1 cannabinoid receptor ligands. *Mini-Rev. Med. Chem.* **2005**, *5*, 631−640.

(23) Papahatjis, D. P.; Nahmias, V. R.; Nikas, S. P.; Andreou, T.; Alapafuja, S. O.; Tsotinis, A.; Guo, J.; Fan, P.; Makriyannis, A. C1′-cycloalkyl side chain pharmacophore in tetrahydrocannabinols. *J. Med. Chem.* **2007**, *50*, 4048−4060.

(24) Papahatjis, D. P.; Nikas, S. P.; Kourouli, T.; Chari, R.; Xu, W.; Pertwee, R. G.; Makriyannis, A. Pharmacophoric requirements for the cannabinoid side chain. Probing the cannabinoid receptor subsite at C1′. *J. Med. Chem.* **2003**, *46*, 3221−3229.

(25) Papahatjis, D. P.; Nikas, S. P.; Andreou, T.; Makriyannis, A. Novel 1′,1′-chain substituted Delta(8)-tetrahydrocannabinols. *Bioorg. Med. Chem. Lett.* **2002**, *12*, 3583−3586.

(26) Nikas, S. P.; Alapafuja, S. O.; Papanastasiou, I.; Paronis, C. A.; Shukla, V. G.; Papahatjis, D. P.; Bowman, A. L.; Halikhedkar, A.; Han, X.; Makriyannis, A. Novel 1′,1′-chain substituted hexahydrocannabinols: 9beta-hydroxy-3-(1-hexyl-cyclobut-1-yl)-hexahydrocannabinol (AM2389) a highly potent cannabinoid receptor 1 (CB1) agonist. *J. Med. Chem.* **2010**, *53*, 6996−7010.

(27) Durdagi, S.; Kapou, A.; Kourouli, T.; Andreou, T.; Nikas, S. P.; Nahmias, V. R.; Papahatjis, D. P.; Papadopoulos, M. G.; Mavromoustakos, T. The application of 3D-QSAR studies for novel cannabinoid ligands substituted at the C1′ position of the alkyl side chain on the structural requirements for binding to cannabinoid receptors CB1 and CB2. *J. Med. Chem.* **2007**, *50*, 2875−2885.

(28) Lu, D.; Meng, Z.; Thakur, G. A.; Fan, P.; Steed, J.; Tartal, C. L.; Hurst, D. P.; Reggio, P. H.; Deschamps, J. R.; Parrish, D. A.; George, C.; Jarbe, T. U.; Lamb, R. J.; Makriyannis, A. Adamantyl cannabinoids: a novel class of cannabinergic ligands. *J. Med. Chem.* **2005**, *48*, 4576−4585.

(29) Petrzilka, T.; Haefliger, W.; Sikemeier, C. Synthese von haschisch-inhaltsstoffen. *Helv. Chim. Acta* **1969**, *52*, 1102−1134.

(30) Thakur, G. A.; Nikas, S. P.; Duclos, R. I., Jr.; Makriyannis, A. Methods for the synthesis of cannabinergic ligands. *Methods Mol. Med.* **2006**, *123*, 113−148.

(31) Chaudhari, S. S.; Akamanchi, K. G. Thionyl chloride−benzotriazole in methylene chloride: a convenient solution for conversion of alcohols and carboxylic acids expeditiously into alkyl chlorides and acid chlorides by simple titration. *Synlett* **1999**, 1763−1765.

(32) Ager, D. J.; Prakash, I.; Schaad, D. R. 1,2-Amino alcohols and their heterocyclic derivatives as chiral auxiliaries in asymmetric synthesis. *Chem. Rev.* **1996**, *96*, 835−876.

(33) Evans, D. A.; Weber, A. E. Asymmetric glycine enolate aldol reactions: synthesis of cyclosporine's unusual amino acid, MeBmt. *J. Am. Chem. Soc.* **1986**, *108*, 6757−6761.

(34) Evans, D. A.; Evrard, D. A.; Rychnovsky, S. D.; Fruh, T.; Whittingham, W. G.; DeVries, K. M. A general approach to the asymmetric synthesis of vancomycin-related arylglycines by enolate azidation. *Tetrahedron Lett.* **1992**, *33*, 1189−1192.

(35) Vanderlei, J. M. L.; Coelho, F.; Almeida, W. P. A stereoselective synthesis of malbranicin. *Tetrahedron: Asymmetry* **1997**, *8*, 2781−2785.

(36) Papahatjis, D. P.; Nikas, S.; Tsotinis, A.; Vlachou, M.; Makriyannis, A. A new ring-forming methodology for the synthesis of conformationally constrained bioactive molecules. *Chem. Lett.* **2001**, 192−193.

(37) Tsotinis, A.; Vlachou, M.; Papahatjis, D. P.; Calogeropoulou, T.; Nikas, S. P.; Garratt, P. J.; Piccio, V.; Vonhoff, S.; Davidson, K.; Teh, M. T.; Sugden, D. Mapping the melatonin receptor. 7. Subtype selective ligands based on beta-substituted *N*-acyl-5-methoxytryptamines and beta-substituted *N*-acyl-5-methoxy-1-methyltryptamines. *J. Med. Chem.* **2006**, *49*, 3509−3519.

(38) Matsuda, L. A.; Lolait, S. J.; Brownstein, M. J.; Young, A. C.; Bonner, T. I. Structure of a cannabinoid receptor and functional expression of the cloned cDNA. *Nature* **1990**, *346*, 561−564.

(39) Abood, M. E.; Ditto, K. E.; Noel, M. A.; Showalter, V. M.; Tao, Q. Isolation and expression of a mouse CB1 cannabinoid receptor gene. Comparison of binding properties with those of native CB1 receptors in mouse brain and N18TG2 neuroblastoma cells. *Biochem. Pharmacol.* **1997**, *53*, 207−214.

(40) Gerard, C.; Mollereau, C.; Vassart, G.; Parmentier, M. Nucleotide sequence of a human cannabinoid receptor cDNA. *Nucleic Acids Res.* **1990**, *18*, 7142.

(41) Shire, D.; Calandra, B.; Delpech, M.; Dumont, X.; Kaghad, M.; LeFur, G.; Caput, D.; Ferrara, P. Structural features of the central

cannabinoid CB1 receptor involved in the binding of the specific CB1 antagonist SR 141716A. *J. Biol. Chem.* **1996**, *271*, 6941−6946.
(42) Shire, D.; Calandra, B.; Rinaldi-Carmona, M.; Oustric, D.; Pessegue, B.; Bonnin-Cabanne, O.; Le Fur, G.; Caput, D.; Ferrara, P. Molecular cloning, expression and function of the murine CB2 peripheral cannabinoid receptor. *Biochim. Biophys. Acta* **1996**, *1307*, 132−136.
(43) Khanolkar, A. D.; Lu, D.; Ibrahim, M.; Duclos, R. I., Jr.; Thakur, G. A.; Malan, T. P., Jr.; Porreca, F.; Veerappan, V.; Tian, X.; George, C.; Parrish, D. A.; Papahatjis, D. P.; Makriyannis, A. Cannabilactones: a novel class of CB2 selective agonists with peripheral analgesic activity. *J. Med. Chem.* **2007**, *50*, 6493−6500.
(44) Mukherjee, S.; Adams, M.; Whiteaker, K.; Daza, A.; Kage, K.; Cassar, S.; Meyer, M.; Yao, B. B. Species comparison and pharmacological characterization of rat and human CB2 cannabinoid receptors. *Eur. J. Pharmacol.* **2004**, *505*, 1−9.
(45) Nikas, S. P.; Grzybowska, J.; Papahatjis, D. P.; Charalambous, A.; Banijamali, A. R.; Chari, R.; Fan, P.; Kourouli, T.; Lin, S.; Nitowski, A. J.; Marciniak, G.; Guo, Y.; Li, X.; Wang, C. L.; Makriyannis, A. The role of halogen substitution in classical cannabinoids: a CB1 pharmacophore model. *AAPS J.* **2004**, *6*, e30.
(46) Hale, J. T.; Bigelow, J. C.; Mathews, L. A.; McCormack, J. J. Analytical and pharmacokinetic studies with 5-chloro-2′-deoxycytidine. *Biochem. Pharmacol.* **2002**, *64*, 1493−1502.
(47) Wood, J. T.; Smith, D. M.; Janero, D. R.; Zvonok, A. M.; Makriyannis, A. Therapeutic modulation of cannabinoid lipid signaling: metabolic profiling of a novel antinociceptive cannabinoid-2 receptor agonist. *Life Sci.* **2013**, *92*, 482−491.
(48) Liang, Q.; Zhang, J.; Quan, W.; Sun, Y.; She, X.; Pan, X. The first asymmetric total syntheses and determination of absolute configurations of xestodecalactones B and C. *J. Org. Chem.* **2007**, *72*, 2694−2697.
(49) Winkler, D. E.; Whetstone, R. R. Some observations on the Pechmann reaction. *J. Org. Chem.* **1961**, *26*, 784−787.
(50) Agurell, S.; Edward, C.; Halldin, M.; Leander, K.; Levy, S.; Lindgren, J. E.; Mechoulam, R.; Nordqvist, M.; Ohlsson, A. Chemical synthesis and biological occurrence of carboxylic-acid metabolites of delta-1(6)-tetrahydrocannabinol. *Drug Metab. Dispos.* **1979**, *7*, 155−161.
(51) Piettre, A.; Chevenier, E.; Massardier, C.; Gimbert, Y.; Greene, A. E. Synthetic approach to hypoxyxylerone, novel inhibitor of topoisomerase I. *Org. Lett.* **2002**, *4*, 3139−3142.
(52) Adams, R.; Harfenist, M.; Loewe, S. New analogs of tetrahydrocannabinol. *J. Am. Chem. Soc.* **1949**, *71*, 1624−1628.
(53) Borne, R. F.; Mauldin, S. C. Synthesis of C-3 side-chain carboxylic-acid cannabinoid derivatives. *J. Heterocycl. Chem.* **1985**, *22*, 693−696.
(54) Adams, R.; Mac, K. S., Jr.; Loewe, S. Tetrahydrocannabinol homologs with double branched alkyl groups in the 3-position. *J. Am. Chem. Soc.* **1948**, *70*, 664−668.
(55) Cheng, Y.; Prusoff, W. H. Relationship between the inhibition constant (K_i) and the concentration of inhibitor which causes 50 per cent inhibition (I_{50}) of an enzymatic reaction. *Biochem. Pharmacol.* **1973**, *22*, 3099−3108.
(56) Paronis, C. A.; Nikas, S. P.; Shukla, V. G.; Makriyannis, A. Delta(9)-Tetrahydrocannabinol acts as a partial agonist/antagonist in mice. *Behav. Pharmacol.* **2012**, *23*, 802−805.
(57) Chang, G.; Guida, W. C.; Still, W. C. An internal coordinate Monte-Carlo method for searching conformational space. *J. Am. Chem. Soc.* **1989**, *111*, 4379−4386.
(58) Saunders, M.; Houk, K. N.; Wu, Y. D.; Still, W. C.; Lipton, M.; Chang, G.; Guida, W. C. Conformations of cycloheptadecane—a comparison of methods for conformational searching. *J. Am. Chem. Soc.* **1990**, *112*, 1419−1427.
(59) *MacroModel*; Schrödinger, LLC: New York, NY, 2012.
(60) Kaminski, G. A.; Friesner, R. A.; Tirado-Rives, J.; Jorgensen, W. L. Evaluation and reparametrization of the OPLS-AA force field for proteins via comparison with accurate quantum chemical calculations on peptides. *J. Phys. Chem. B* **2001**, *105*, 6474−6487.
(61) Still, W. C.; Tempczyk, A.; Hawley, R. C.; Hendrickson, T. Semianalytical treatment of solvation for molecular mechanics and dynamics. *J. Am. Chem. Soc.* **1990**, *112*, 6127−6129.
(62) Dixon, D. D.; Sethumadhavan, D.; Benneche, T.; Banaag, A. R.; Tius, M. A.; Thakur, G. A.; Bowman, A.; Wood, J. T.; Makriyannis, A. Heteroadamantyl cannabinoids. *J. Med. Chem.* **2010**, *53*, 5656−5666.